

C01 and PC01

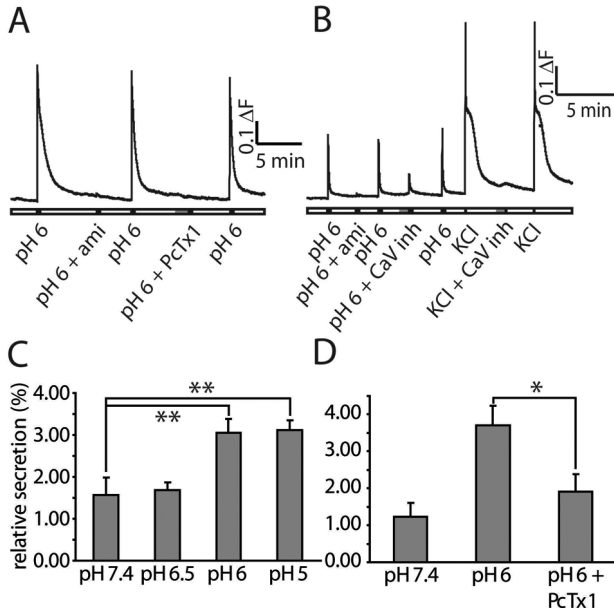
Role of Acid-sensing ion channels (ASICs) in neuropeptide secretion from sensory neurons

A. Boillat and S. Kellenberger

Department of Pharmacology and Toxicology, University of Lausanne, Lausanne, Switzerland

Acid-sensing ion channels (ASICs) are non-voltage-gated sodium channels activated by an extracellular acidification. They are widely expressed in neurons of the central and peripheral nervous system. Tissue damage leads to the release of inflammatory mediators. This so called inflammatory soup includes, among different signalling molecules, serotonin, histamine, glutamate, ATP and protons. Isolectin B4-negative neurons are able to release neuropeptides calcitonin gene-related peptide (CGRP) and substance P (SP). Neurogenic inflammation refers to the process whereby peripheral release of the neuropeptides, CGRP and SP, induces vasodilation and extravasation of plasma proteins, respectively. Our laboratory has previously shown that calcium-permeant homomeric ASIC1a channels are present in a majority of IB4 negative, CGRP- and SP-positive small diameter sensory neurons (Poirot et al., 2006). We hypothesize that a local acidification can produce an ASIC-mediated calcium-dependant neuropeptide secretion.

To test this hypothesis we have first verified the co-expression of ASIC1 and CGRP/SP using immunochemistry on dissociated rat dorsal root ganglion (DRG) neurons. We found that most CGRP/SP-positive neurons also expressed ASIC1a subunits. Calcium imaging experiments with fura-2 AM dye showed that an extracellular acidification can induce an increase of intracellular Ca^{2+} concentration, which is essential for secretion. This increase of intracellular Ca^{2+} concentration is, at least in some cells, ASIC dependant, as it can be prevented by Amiloride, a non-specific ASIC antagonist and by Psalmotoxin (PcTx1), a specific ASIC1a antagonist. Voltage-gated calcium (CaV) channels also play an important role. CaV inhibitors (ω -conotoxin MVIIC, Mibefradil and Nifedipine) reduce the Ca^{2+} increase in amiloride sensitive neurons during an acidification to pH 6. Secretion assay results show that CGRP secretion can be induced by extracellular acidification in cultured rat DRG neurons. PcTX1 reduced the acidification-induced CGRP secretion, suggesting that homomeric ASIC1a may play a key role in this process. Taken together, these results show that in our in vitro model a mild extracellular acidification can induce a calcium-dependant neuropeptide secretion. In conclusion, in a subpopulation of DRG neurons, this secretion is mediated by ASICs, and especially ASIC1a channels, even if we can not totally exclude the involvement of TRPV1, the other major acid sensitive channel present in DRG neurons.



Extracellular acidification increases intracellular Ca^{2+} concentration and CGRP secretion.

A-B: Calcium imaging experiments in rat DRG neurons. A: Amiloride (500 μM) and PcTx1 (10 nM) prevent intracellular calcium increase by extracellular acidification. B: Voltage-gated calcium channel inhibitors decrease acidification-induced Ca^{2+} -entry. C-D: CGRP secretion assay in cultured rat DRG neurons at 37°C, 15 minutes of secretion. Quantity of CGRP is measured with an enzyme immunoassay. Values are expressed relative to the total cellular CGRP content. C: extracellular acidification increases CGRP secretion. D: PcTx1 (10 nM) inhibits CGRP secretion activated by extracellular acidification. Statistics: **:P<0.01, *:P<0.05, unpaired t-test.

Poirot O et al. (2006). J Physiol 576, 215-234.

Where applicable, the authors confirm that the experiments described here conform with The Physiological Society ethical requirements.

C02 and PC02

The molecular and cellular identity of peripheral osmoreceptors

S.G. Lechner¹, S. Markworth¹, K. Poole¹, E.S. Smith¹, L. Lapatsina¹, F.C. Luft³, J. Jordan² and G.R. Lewin¹

¹Max-Delbrueck-Centre for Molecular Medicine, Berlin, Germany, ²Institute for Clinical Pharmacology, Medical School Hannover, Hannover, Germany and ³ECRC, Charite, Berlin, Germany

The osmolality of the extra cellular body fluid (ECF) is subject to permanent changes due to salt/water intake and excretion. As large deviations from the normal osmolality have fatal effects on the physical and functional integrity of cells and tissues, afferent systems have evolved that detect hypo- or hyperosmotic shifts in the ECF and trigger homeostatic control to keep osmolality at a well defined physiological set point. It had previously been suggested, that in addition to central osmoreceptors, peripheral osmoreceptors might exist which could contribute to the regulation of ECF osmolality. Here we show that oral administration of 1ml of water in awake mice causes a drop in blood osmolality (-8%) in the liver portal vein (for blood sampling mice were anaesthetised by i.p. injection of 0.3ml PBS containing 10mg/ml Ketavet and 0.04% ROMPUN), which results in the activation of pERK (phosphorylated form of ERK) in hepatic afferent endings from thoracic DRG neurons. We quantified pERK immunoreactivity in sensory fibers around blood vessels as this is a reliable marker of neuronal activation. Fura-2 calcium imaging experiments on thoracic neurons showed that osmosensitive neurons are enriched in these ganglia (33%, n=167). We further show that the hypo-osmotically induced calcium transients occur concurrently with cell swelling and depend on extracellular Ca²⁺, but are not affected by depletion of intracellular calcium stores with thapsigargin or by blockade of voltage-gated calcium channels with Cadmium. Patch-clamp recordings with simultaneous fura-2 imaging revealed that a non-selective outwardly rectifying cation channel, which is half-maximally activated at ~278mOsm, mediates the increases in intracellular calcium. Electrophysiological experiments on retrogradely labelled sensory neurons that project to the liver revealed that almost all thoracic liver afferents are osmosensitive (20/23), but none of the vagal hepatic afferents in the nodose ganglia, are osmosensitive (0/16). Members of the transient receptor potential (TRP) ion channel family, in particular TRPV1 and TRPV4, have been suggested to play a role in osmosensing and consistently the TRP channel blockers Ruthenium Red and Gd³⁺ abolished calcium transients and osmosensitive inward currents in thoracic sensory neurons. Using qRT-PCR we could show that TRPV4 mRNA is enriched in thoracic DRGs and immunostaining of liver sections confirmed that TRPV4 is present at the peripheral nerve endings of hepatic afferent fibres. Strikingly, in mice lacking TRPV4, hepatic sensory neurons no longer exhibit osmosensitive inward currents and the in-vivo activation of liver afferents following water intake is abolished.

Taken together we have identified a new population of thoracic sensory neurons that serve as peripheral osmoreceptors and show that they require the osmosensitive ion channel TRPV4 to sense small ongoing changes in hepatic blood osmolality.

This work was supported by an internal clinical cooperation grant from the MDC and ECRC and the DFG/SFB 665.

Where applicable, the authors confirm that the experiments described here conform with The Physiological Society ethical requirements.

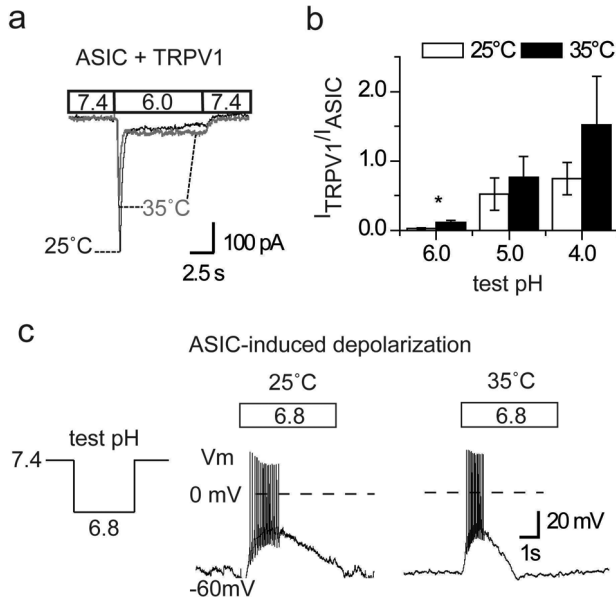
C03 and PC03

Effect of a temperature increase in the non-noxious range on proton-evoked ASIC and TRPV1 activity

M.G. Blanchard and S. Kellenberger

Pharmacology and Toxicology, University of Lausanne, Lausanne, Switzerland

Acid-sensing ion channels (ASICs) are neuronal H⁺-gated cation channels, and the transient receptor potential vanilloid 1 channel (TRPV1) is a multimodal cation channel activated by low pH, noxious heat, capsaicin, and voltage. ASICs and TRPV1 are both expressed in sensory neurons (1). It has been shown that raising the temperature increases TRPV1 and decreases ASIC H⁺-gated current amplitudes (2). To understand the underlying mechanisms, we have analyzed ASIC and TRPV1 function in a recombinant expression system and in rat dorsal root ganglion (DRG) neurons at room and physiological temperature (25 and 35°C). We show that in this range, the temperature does not affect the pH dependence of ASIC and TRPV1 activation. A temperature increase induces, however, a small alkaline shift of the pH dependence of steady-state inactivation of ASIC1a, ASIC1b, and ASIC2a. The decrease in ASIC peak current amplitudes at higher temperatures is likely in part due to the observed accelerated open channel inactivation kinetics and for some ASIC types to the changed pH dependence of steady-state inactivation. The increase in H⁺-activated TRPV1 current at the higher temperature is at least in part due to a hyperpolarizing shift in its voltage dependence. ASIC and TRPV1 currents of DRG neurons are similarly regulated by temperature as the cloned channels, with the exception that the decrease in peak ASIC current amplitudes at 35°C is more pronounced in DRG neurons. The low pH-evoked depolarization measured under current-clamp was significantly reduced at 35°C for a sub-population of ASIC channels, without however affecting the number of action potentials. Our study shows that the contribution of TRPV1 relative to ASICs to H⁺-gated currents in DRG neurons increases with higher temperature and acidity. Still, ASICs remain the principal pH sensors of DRG neurons at 35°C in the pH range ≥ 6 .



Patch clamp experiments were performed in rat DRG neurons expressing ASIC and TRPV1 channels. a) ASIC and TRPV1 are differentially modulated by temperature. Increasing the temperature from 25 to 35°C reduced ASIC pH 6-evoked current while increasing TRPV1 activity. b) ASIC currents were larger than TRPV1 at both 25 and 35°C at pH>=6. c) Higher temperature increased the frequency of low pH-evoked action potentials but did not affect the number of spikes.

Poirot O et al. (2006). J Physiol 576(Pt 1), 215-234.

Neelands TR et al. (2010). Brain Res 1329, 55-66.

Where applicable, the authors confirm that the experiments described here conform with The Physiological Society ethical requirements.

C04 and PC04

Mechoreceptor firing threshold – A continuum mechanics study

M.E. Mickael¹, A. Heydari^{2,1}, R.S. Crouch¹, S. Pyner² and S. Johnstone¹

¹*School of Engineering and Computing Sciences, Durham University, Durham, UK and*

²*Biological and Biomedical Sciences, Durham University, Durham, UK*

The research investigates whether the location of mechanoreceptors contributes to the firing threshold using a continuum mechanics approach. Baroreceptors, situated in the media and adventitia of arterial walls, are considered. Histological studies have shown the media is elastically softer than the adventitia (J Levick, 2003). The main materials constituting these layers are elastin (elastically soft), collagen

(elastically stiffer) and smooth muscle cells. Only the passive stress-strain relationship of elastin and collagen are considered in this study. Baroreceptors are classified as A- and C-fibres (Holzapfel et al., 2005). A-fibres are myelinated resulting in higher spike conduction speeds, whereas C-fibres are unmyelinated and slower. A-fibres have a conduction range in the region of 30-90 mmHg whilst type C has a range of 70-140 mmHg (J Levick, 2003).

The relationship between blood pressure and strain energy, defined as the potential energy passively stored in a layer as a function of strain, in individual layers of a coronary arterial wall is explored. This is used to test the assumption that the threshold and sensitivity of the mechanoreceptor firing rate are affected by the stiffness of the tissue in which they are embedded.

Mathematical models based on an empirically derived strain energy formulation were constructed for all three arterial layers, assuming a concentric cylindrical geometry. Each layer model incorporated factors such as heterogeneity, anisotropy, and collagen fibre angle. The same form was used for each layer, but with different material parameters. These were optimised using a Monte Carlo method using constraints defined by histological data and stress equilibrium (ME Mickael A Heydari, RS Crouch et al., 2010).

The strain energy as a function of blood pressure for the adventitia and media of a coronary artery is shown in Figure 1. This shows that for a given blood pressure the adventitia stores more strain energy than the media (ME Mickael, A Heydari, S Pyner et al., 2010). Considering the case of baroreceptors with identical firing thresholds (eg 1kJ) located in both these layers, the model predicts that the receptors in the adventitia would fire at a lower blood pressure (e.g. ~30mmHg) than those in the media (e.g. ~65mmHg). Similarly, if both receptors have the same saturation strain energy threshold, those in the adventitia saturate whereas those in the media have a much extended range. Thus the evidence suggests that receptors in the adventitia behave similarly to A-fibres whereas those in the media as C-fibres. Thus, this study concludes that it is theoretically possible for the location of a mechanoreceptor to affect the firing thresholds when expressed in terms of blood pressure.

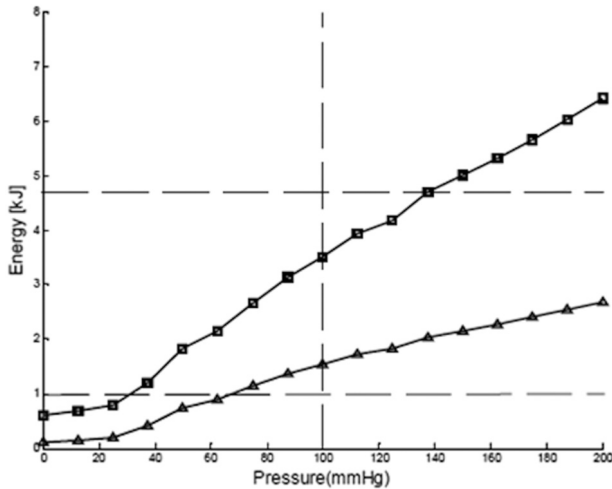


Figure1: Estimated strain-energy for the adventitia (squares) and media (triangle) as a function of luminal blood pressure for a coronary artery

J. Levick, 5th Ed, London: Hodder Arnold, 2009.

GA Holzapfel, et al., Am. J. Physiol. Heart Circ. Physiol., 289, H2048-2058, 2005.

ME Mickael, A Heydari, RS Crouch et al., Proc. of Comp. in Card., Sept. 2010.

ME Mickael, A Heydari, S Pyner et al., "Appl. Bion. and Biomech.", ICABB-2010, Oct. 2010

We gratefully acknowledge EPSRC for funding.

Where applicable, the authors confirm that the experiments described here conform with The Physiological Society ethical requirements.

C05 and PC05

Down-regulation of small-conductance Ca^{2+} -activated K^+ channels (SK3) in the pregnant human myometrium weeks before term

M. Rahbek^{1,2}, S.T. Rosenbaum³, D.A. Klaerke¹, L. Ødum², T. Larsen⁴ and P. Bouchelouche³

¹Department of Physiology and Biochemistry, IBHV, Copenhagen University, Copenhagen, Denmark, ²Department of Clinical Biochemistry, Roskilde Hospital, Roskilde, Denmark, ³Smooth Muscle Research Centre, Koege Hospital, Koege, Denmark and ⁴Department of Gynaecology, Holbaek Hospital, Holbaek, Denmark

Introduction Small-conductance Ca^{2+} -activated K^+ channels (SK channels) have been described in the myometrium from non-pregnant humans, and the expression of the channels has been shown to be down-regulated in pregnancies at term

(1,2,3). It has been suggested that expression of SK channels may be important for the relaxation of the myometrium during pregnancy, and decreased expression may be a prerequisite for contractions required at delivery. The aim of our study was to investigate the expression of the SK channel isoforms SK2 and SK3 in human pregnant myometrium in term and in preterm deliveries.

Materials and methods Human myometrial tissue was obtained in connection with hysterectomy from non-pregnant women (NP) and from pregnant women during caesarean section at term (late pregnant (LP), 38-42 weeks of gestation) and at preterm deliveries (preterm (PT) 27-32 weeks of gestation). Expression of SK2 and SK3 (mRNA levels) were determined by qPCR as ratio to β -actin. Western Blot was used to investigate the channel expression at the protein levels.

Results qPCR showed a significantly lower expression of SK2 gene in non-pregnant myometrium as compared to SK3 (normalized value of SK3 was set to 1.00 ± 0.23 (mean \pm S.E.M) and that of SK2 was found to be 0.081 ± 0.002 , $p = 0.0005$, using Mann-Whitney U test, $n = 9$ and 11 for SK2 and SK3 respectively). The level of SK2 mRNA showed no significant change in the pregnant tissue compared to the non-pregnant ($p = 0.673$ using Mann-Whitney U test, $n = 11$ and 8 for NP and LP respectively). This was confirmed on protein-level with western blot ($n = 4$ for NP and LP). The expressions of SK3 gene in late pregnant and pregnant with preterm deliveries were both significantly lower than the expression in non-pregnant (normalized expression of 0.152 ± 0.002 for PT and 0.132 ± 0.026 for LP. Tested with Mann-Whitney U test, $p = 0.0127$ for NP versus PT, and $p = 0.0005$ for NP versus LP, $n = 11$, 5 and 12 for NP, PT and LP respectively). This was confirmed on protein level ($n = 4$ for NP and LP).

Conclusion The present study shows that SK3 is the dominant SK isoform in the human myometrium. The level of SK2 expression is insignificant as compared to the level of SK3 in the non-pregnant tissue. The expression of SK3 is strongly down-regulated during the time of delivery in term, but surprisingly the down-regulation appears to take place sometime before week 27 to 32. This indicates that SK3 is not contributing to the relaxation of the myometrium in the last weeks of pregnancy.

Mazzone J et al. (2003) Proc. West. Pharmacol Soc. 46: 74-77

Mazzone J et al. (2002) Proc. West. Pharmacol. Soc. 45: 184-186

Pierce SL & England SK. (2010) Am J Physiol Endocrinol Metab 299, E640-646

Where applicable, the authors confirm that the experiments described here conform with The Physiological Society ethical requirements.

C06 and PC06

Target-specific siRNA to protein kinase C delta isoform gene expression normalizes vascular function in SHR

T. Novokhatska¹, I. Ivanova¹, S. Tishkin¹, V. Dosenko² and A. Soloviev¹

¹*Experimental therapy, Institute of pharmacology and toxicology of AMS, Kiev, Ukraine* and ², *Bogomoletz Institute of Physiology of NAS, Kiev, Ukraine*

It is known that protein kinase C (PKC) family plays an important role in hypertension development, cardiac hypertrophy and the subsequent heart failure (Soloviev, Bershtein, 1992, Jalili et al. 1999, Wang et al. 2003). PKC activation leads to myocyte growth and heart contractility (Naruse et al. 2000). The vascular smooth muscle (SM) tone is closely coupled to membrane potential, which, in turn, is determined by K⁺ channels activity. Potassium conductance is altered in both radiation-induced (Soloviev et al. 2009) and essential hypertension (Cox et al. 2001). Thus, high PKC activity is a common distinctive feature for arterial hypertension development.

The goal of this study was to identify the most vulnerable target for pharmacological interventions in arterial hypertension. The experimental design of the study comprised patch-clamp technique, RT-PCR and standard ACh test.

We measured the level of δ -PKC gene expression in thoracic aorta from SHR and SHR treated with δ -PKC siRNA relative to control rats (via tail vein under ketamine (45mg/kg, i.p.) and xylazine (10 mg/kg, i.p. anaesthesia). The RT-PCR analysis showed that the PKC- δ -isoform mRNA expression is sixfold increased in SMCs from SHR and was significantly higher than seen in SHR treated with δ -PKC siRNA (control, 11.8 ± 1.71 , n=6; SHR, 43.61 ± 6.32 , n=6; SHR treated with δ -PKC siRNA, 33.76 ± 1.28 , n=6; p<0.05). The BKCa component of outward current is significantly decreased from 48 ± 5 pA/pF in healthy rats to 25 ± 2 pA/pF in SHR while in SHR treated with δ -PKC siRNA it was 35 ± 3 pA/pF, P<0.05, n=18. The target-specific to δ -PKC siRNA administration led to an increment in amplitude of ACh-relaxation and BKCa activity, and promoted arterial blood pressure normalization in SHR.

In conclusion, δ -PKC gene silencing restores endothelium-dependent relaxation and BKCa channels function in vascular SHR SM cells. It is likely that siRNA is a good approach to inactivate PKC gene encoding function and to normalize vasodilator potential in SHR.

Where applicable, the authors confirm that the experiments described here conform with The Physiological Society ethical requirements.

C07 and PC07

Primary cilia are necessary for cartilage mechanotransduction

A.K. Wann¹, S.R. McClashan², C.J. Haycraft³, C.A. Poole⁴ and M.M. Knight¹

¹Cell and Tissue Engineering, Queen Mary, London, UK, ²Department of Anatomy with Radiology, University of Auckland, Auckland, New Zealand, ³Department of Craniofacial Biology, Medical University of South Carolina, Charleston, SC, USA and ⁴Department of Medicine, University of Otago, Otago, New Zealand

Chondrocytes within articular cartilage respond to mechanical loading by adjusting the synthesis of extracellular matrix components such as collagen type II and the proteoglycan, aggrecan. This occurs via a mechanotransduction pathway which involves the release of ATP and activation of Ca^{2+} signalling^[1,2]. Chondrocytes possess primary cilia, which in other cell types function as mechanoreceptors^[3]. This study tests the hypothesis that chondrocyte primary cilia are required for mechanosensitive ATP release and up-regulation of matrix synthesis.

Articular chondrocytes derived from Wild-type (WT) and *Tg737* Oak Ridge Polycystic Kidney (ORPK) mice were cultured in 3D agarose constructs. Mutation of the *Tg737* gene (IFT88) disrupts polaris expression, halting ciliogenesis. Cilia expression was studied by confocal immunofluorescence of acetylated α -tubulin. Cell-agarose constructs were subjected to mechanical loading at 1Hz and 0-15% compressive strain for 1 hour. ATP release was quantified by the luciferase assay and the expression of collagen II and aggrecan assessed by qPCR. To investigate proteoglycan production at a protein level, constructs were subjected to 24 hours of cyclic compression followed by quantification of sulphated glycosaminoglycan (sGAG) using a spectrophotometric biochemical assay.

Primary cilia were present in WT chondrocytes but there was an almost complete absence in ORPK cells. Both cell types expressed collagen II and aggrecan genes and synthesised sGAG. However, in the unloaded state, ORPK cells exhibited increased aggrecan gene expression ($p < 0.0001$, $n = 12$) but reduced sGAG production ($p < 0.0001$, $n = 36$) compared to WT cells. There was no difference in the basal level of ATP secretion. Mechanical loading had no effect on viability or proliferation for either cell type. However for WT cells, loading increased ATP release ($p < 0.01$, $n = 35$), increased aggrecan gene expression ($p < 0.05$, $n = 9$) and increased sGAG production ($p < 0.05$, $n = 36$). By contrast, this mechanically induced proteoglycan synthesis was absent in ORPK cells, although these cells maintained mechanically-induced ATP secretion ($p = 0.001$, $n = 35$). Unpaired T-tests or Mann-Whitney U-tests were used as appropriate.

To conclude, ORPK chondrocytes without cilia show disrupted basal proteoglycan production with a complete loss of mechanosensitive up-regulation of aggrecan expression and sGAG synthesis. However the loss of cilia did not influence the ATP response, indicating that cilia are involved in chondrocyte mechanotransduction downstream of mechanosensitive release of ATP. For example, this may involve Ca^{2+} dependent modulation of the P2 receptors. These experiments provide the first evi-

dence that the primary cilium is central to chondrocyte matrix synthesis and mechanotransduction with fundamental implications for both healthy and arthritic tissue. Chowdhury, T.T. and M.M. Knight, Purinergic pathway suppresses the release of .NO and stimulates proteoglycan synthesis in chondrocyte/agarose constructs subjected to dynamic compression. *J Cell Physiol*, 2006. 209(3): p. 845-53.

Garcia, M. and M.M. Knight (2010). Cyclic loading opens hemichannels to release ATP as part of a chondrocyte mechanotransduction pathway. *J Orthop Res*. 28(4): p. 510-5.

Hovater, M.B., et al., Loss of apical monocilia on collecting duct principal cells impairs ATP secretion across the apical cell surface and ATP-dependent and flow-induced calcium signals. *Purinergic Signal*, 2008. 4(2): p. 155-70.

A. Wann is supported by the Wellcome Trust, UK.

Where applicable, the authors confirm that the experiments described here conform with The Physiological Society ethical requirements.

C08 and PC08

Spirostomum Ambiguum: A Protozoan Model for Primordial Musculoskeletal Exchange?

P.E. Garner, V. Fallon and J.E. Aaron

FBS, University of Leeds, Leeds, West Yorkshire, UK

The skeleton is responsive to mechanical usage (immobility means significant atrophy), yet the basis for its remarkable sensitivity remains uncertain. Osteocytes seem central as they are the most abundant bone cells (90%). Their cytoplasmic syncytium is pervasive and well placed to bridge the uncertain gap between mechanical signal transduction and cellular response especially since it is morphologically reminiscent of a neuronal network. However, its calcified entombment limits accessibility, while isolation or manipulation may alter its specific threshold characteristics. Insight into the basics of musculoskeletal exchange may be found in certain protozoa from which the metazoan pathway apparently evolved (Pautard, 1960, 1970; Ruffalo, 1978). In particular is the organism *Spirostomum ambiguum* (a cigar-shaped creature visible to the naked eye) which fabricates and accumulates calcium phosphate particles, about 1 μm in diameter, resembling those in bone. Moreover, their intracellular, golgi-directed synthesis (Fallon and Aaron, in press) is determined by the active life-cycle of the animal. This modulates between a free-swimming state when calcified particles are minimal and a silt-burrowing stage when calcified particles become abundant. Thus when the mineral of cultured *S. ambiguum* was labelled with the fluorochrome tetracycline (commonly used as a bone histology marker of formation) the green fluorescence intensity (AU) mapped using laser confocal microscopy, recorded a high mineral level in the silt-burrowing animals ($138.0 \pm \text{SD}4.0$) compared with their free-swimming counterparts ($89.7 \pm \text{SD} 3.3$). Similarly when the live organisms were transfected with a GFP construct (Fallon, 2006) the resulting GFP-tagged mannosidase II enzyme as an expression of Golgi activity

differed significantly ($p < 0.0001$, two-sample t-test) between tunnelling ($104.6 \pm \text{SD } 2.7$) and free-swimming (74.5 ± 6.7) activity. Within the same context, it was observed that the distribution of the intracellular particles did not seem to be entirely random. Rather, a proportion related in disposition to a regular and well-defined pattern of contractile muscle myonemes, the fibres of which were arranged longitudinally within the high stress burrowers in contrast to their transverse alignment in the low stress swimmers. The capacity of this animal model not only to package bone-like mineral in response to changing environmental pressures, but also to relate them to their intracellular contractile elements may suggest an early integrated musculoskeletal system and cytoplasmic calcium phosphate storage phenomenon that substantially predated the vertebrates which eventually exploited the major advantages they bestowed. The apparently modest protozoan model described may therefore serve as a valuable tool for future fundamental investigation of osteocyte ancestry, mechanotransduction, perception and response.

Pautard, F.G.E. (1960). *Calcification In Biological Systems*. Ed. Sognnaes, R.F. American Society of Advanced Science, Washington D.C. 1.

Pautard, F.G.E. (1970). *Biological Calcification; Cellular and molecular aspects*. North-Holland publishing company, Amsterdam. 105-201.

Ruffolo, J.J., JR. (1978). *Transactions of the American Microscopical Society*, **97**(3), 381-386.

Fallon, V. (2006). PhD Thesis, University of Leeds, UK.

Where applicable, the authors confirm that the experiments described here conform with The Physiological Society ethical requirements.

C09 and PC09

Mechanically evoked spinal reflexes are augmented in a rat model of osteoarthritic pain

S. Kelly¹, G. Allen² and J. Harris²

¹Arthritis Research UK Pain Centre, School of Biosciences, University of Nottingham, Nr Loughborough, UK and ²School of Biosciences, University of Nottingham, Nr Loughborough, UK

Osteoarthritis (OA) is a degenerative joint disease that leads to chronic pain; the mechanisms of which are unclear. OA patients show an expanded original pain area and hyperalgesia at distant sites (Arendt-Nielsen et al., 2010). The monoiodoacetate (MIA) rat model of OA (Bove et al., 2003) is associated with both joint pain and hypersensitivity of distal sites (hind-paw). It is possible that central sensitization underlies the behavioural hypersensitivity in this model, and human OA pain. Indeed, lower limb spinal reflex responses are augmented in human OA knee pain (Courtney et al., 2009, 2010). We have investigated whether spinal reflexes are sensitized in the MIA model.

MIA (1mg/50microl; n=7) or saline (50microl; n=7) was injected intra-articularly (left knee) of male wistar rats under isoflurane anaesthesia (3% in O₂). 28 days post-

MIA/saline, rats were re-anesthetised (induction - 3% isoflurane in N₂O/O₂; maintenance - alfaxan 1.3ml/hr, iv) for recording of ipsilateral hindlimb reflexes (Clarke and Harris 2004). Reflexes were evoked by hindpaw mechanical stimulation with von Frey monofilaments (3s each) or by electrical stimulation at the heel or toes. Hindpaw receptive fields of tibialis anterior (TA, ankle flexor) and biceps femoris (BF, knee flexor) reflexes were mapped (60g von Frey). Then the mechanical threshold and stimulus response function (4-60g von Frey) of TA and BF reflexes were ascertained. The electrical threshold to evoke reflexes in TA, BF and medial gastrocnemius (MG, ankle extensor) as well as the reflex latency were measured. Finally, 'wind-up' of reflexes was studied (8 stimuli, 1 Hz, 1 ms, 10 mA).

MIA resulted in reduced ipsilateral weight bearing (day 3-28; $p < 0.001$; two-way ANOVA). The hindpaw receptive field size for TA and BF reflexes showed a tendency to decrease and increase respectively in MIA rats compared to saline rats. BF hindpaw mechanically evoked reflexes were facilitated in MIA rats compared to saline rats. The threshold was significantly reduced (median = 15 vs 60g, MIA vs saline, $p < 0.05$, Mann Whitney) and the stimulus response curve was significantly augmented ($p < 0.05$, two-way ANOVA, MIA vs saline). No significant differences were observed in electrical thresholds and latencies of spinal reflexes in MIA compared to saline rats. However, the wind-up of the C-fibre component of reflexes to repetitive electrical stimulation appeared to be increased in MIA rats.

We report that the excitability of spinal nociceptive reflexes is increased in a model of OA pain. The facilitation of reflex responses is thought to represent the physiological basis in the motor system for allodynia and hyperalgesia indicating that central sensitization is likely to be responsible at least in part for the pain behaviour exhibited.

Arendt-Nielsen L, et al (2010). Pain. In press.

Bove SE, et al (2003). Osteoarthritis Cartilage. 11, 821-830.

Courtney CA, et al (2009). J Pain. 10, 1242-1249.

Courtney CA, et al (2010). J Pain 11, 179-185.

Clarke RW, Harris J (2004). Brain Res Brain Res Rev 46, 163-172.

This work was funded by the Pain Relief Foundation and a BBSRC Undergraduate Vacation Scholarship.

Where applicable, the authors confirm that the experiments described here conform with The Physiological Society ethical requirements.

C10 and PC10

The physiological basis of acid insensitivity in the African naked mole rat

E. St. John Smith, D. Omerbasic, G. Anirudhan, S.G. Lechner and G.R. Lewin

Dept. of Neuroscience, Max-Delbrück Centre for Molecular Medicine, Berlin, Germany

Nociceptors are somatic sensory neurons activated by noxious stimuli. Perhaps uniquely among mammals, the African naked mole-rat (NMR, *Heterocephalus glaber*) displays neither nocifensive behaviour to acid, nor possesses acid-sensitive C-fibre nociceptors (Park et al. 2008, Smith and Lewin 2009). Insensitivity to acid could be explained by a lack of expression of proton-gated ion channels, which we investigated using whole-cell patch clamp to measure proton-gated currents in nociceptor cell bodies (isolated from the dorsal root ganglia, DRG). By recording from NMR sensory neurones we observed that pH5 evoked transient inward currents in 32% of DRG neurones (peak current density: 52 ± 11 pA/pF, $n=22$) and sustained inward currents in the remaining 68% (32 ± 9 pA/pF, $n=36$). We observed similar, but smaller, currents in mouse DRG neurones (*Mus musculus*): 15% transient (12 ± 3 pA/pF, $n=11$) and 85% sustained (19 ± 4 pA/pF, $n=63$). We next cloned two NMR ion channels, which are proton-sensitive, present in DRG neurons and thought to play a role in acid-mediated pain, transient receptor potential vanilloid 1 (TRPV1) and acid-sensing ion channel 1a (ASIC1a). Both nmrTRPV1 and nmrASIC1a exhibit a similar pH_{50} compared to other rodent TRPV1s and ASIC1as (nmrTRPV1 = $pH_{50} 5.50$ and nmrASIC1a = $pH_{50} 5.64$). Interestingly, in DRG neurones proton-gated inward currents did not correlate with action potential (AP) generation as examined in current-clamp, pH5 evoked APs in only 6% of mouse neurones ($n=49$) and only 19% of NMR neurones. Although acid causes depolarisation, subsequent AP initiation is mediated by voltage-gated sodium channels (NaV) that are inhibited by acid. Total voltage-gated inward currents in mouse DRG neurones were indeed inhibited by acid ($IC_{50} = 5.97$) and pH6 inhibited G_{max} by 45%. Furthermore, using the *in-vitro* skin-nerve preparation, the spike rate of mechanically evoked APs in mouse C-fibre nociceptors was also inhibited over time by a pH4.0 solution to ~50% of control levels. NaV currents mediate the bulk of voltage-gated inward current in DRG neurones and pH6 inhibited isolated NaV current G_{max} by 46%. Interestingly, voltage-gated inward currents in NMR DRG neurones are significantly more sensitive to acid: pH6 caused 63% inhibition (significantly different from in the mouse, $p < 0.01$, Mann Whitney test). Greater inhibition of NMR NaVs may explain their lack of acid-induced nocifensive behaviour. Thus acid induces inward currents in NMR nociceptors, but larger NaV inhibition compared to mouse prevents AP generation. In conclusion, proton-evoked currents are present in NMR DRG neurones, but voltage-gated inward currents are more sensitive to acid-inhibition, which may explain the lack of acid-induced nocifensive behaviour in NMRS.

Park, T. J. et al. (2008) Selective Inflammatory Pain Insensitivity in the African Naked Mole-rat (*Heterocephalus glaber*). *PLoS Biol.*, **6**, e13

Smith, E. St. J. and Lewin, G. R. (2009) Nociceptors: a phylogenetic view. *J. Comp. Physiol. A* **195**, 1089 – 1106.

E. St. J. S. acknowledges the support of an Alexander von Humboldt foundation fellowship.

Where applicable, the authors confirm that the experiments described here conform with The Physiological Society ethical requirements.

C11 and PC11

Defining the forces required to gate mechanosensitive channels in mammalian sensory neurons

K. Poole and G.R. Lewin

Dept. Neuroscience, Max Delbrück Center, Berlin-Buch, Germany

Our sense of touch and mechanical pain is based on mechano-electrical transduction at the terminal endings of dorsal root ganglion (DRG) neurones innervating the skin. How this transduction works, and the molecules responsible have proven difficult to elucidate, due to inaccessibility of the nerve endings and the presumed limited quantity of transduction molecules. Sensory DRG neurones can be acutely prepared and retain mechanosensitivity when cultured on laminin, as determined using whole-cell patch-clamp during direct mechanical stimulation of the neurites or soma. However, such an approach does not allow determination of the precise forces required to gate transduction channels. In order to quantify the stimulus strengths required to gate mechanosensitive channels in these neurons, we have developed an approach using microstructured surfaces. We cast pillar arrays from PDMS, the pillar tips are coated with laminin and then DRG neurones can be cultured on top. Each pilus has a defined elasticity (2 ± 0.1 MPa) and shape ($r = 0.7 \mu\text{m}$; $l = 5 \mu\text{m}$ or $8 \mu\text{m}$), and as such a calculable spring constant. Cells were cultured on top of pili with a calculated spring constant of either 2.2 pN/nm or 9.0 pN/nm. Neurons cultured on pili with a calculated spring constant of 2.2 pN/nm did not extend neurites, in contrast to cells cultured on the stiffer pili. To apply mechanical stimuli, individual pili underneath the neurites are deflected using a piezo-driven nano-manipulator and the deflection is monitored using light microscopy. As the PDMS pili behave as light-guides, the center of the each pilus can be determined from a 2-D Gaussian fit of the intensity, allowing detection of movements as small as a couple of nanometers. The cellular response to the pili deflection is monitored using whole-cell patch-clamp to record the latency, kinetics and amplitude of mechanically gated currents. We show that pili deflections as small as 5 nm can gate the rapidly-adapting current in mechanoreceptor cells, while larger deflections (above 150 nm) are required for gating of slowly-adapting currents in nociceptors. Application of mechanical stimuli via pili deflection resulted in a lower threshold for gating of the rapidly-adapting current (5 nm), compared with application of the stimulus to the top of the neurite (minimum required movement for channel gating = 70-100 nm¹). This suggests that gating occurs at the cell-substrate inter-

face. We have also observed that the latency of activation of rapidly-adapting currents in mechanoreceptors ($293 \pm 1 \mu\text{s}$, $n = 31$) is significantly faster ($p < 0.001$, Mann-Whitney test) than the latency of activation of the same type of current in nociceptors ($548 \pm 13 \mu\text{s}$, $n = 18$). Using such a method we are currently characterising the precise physical conditions, in terms of deflection and applied force, required for mechanotransduction in sensory neurons.

Hu J & Lewin GR (1996). *J Physiol* **577**, 815-828

Where applicable, the authors confirm that the experiments described here conform with The Physiological Society ethical requirements.

C12 and PC12

Combining Scanning Probe and Confocal Microscopy: A new method for studying the Primary Cilium

S. Kocher¹, D.N. Sheppard² and T.J. McMaster¹

¹*School of Physics, University of Bristol, Bristol, UK* and ²*School of Physiology and Pharmacology, University of Bristol, Bristol, UK*

Primary cilia are non-motile specialised mechano-sensory organelles that protrude from the surface of epithelial cells. In the kidney, they are 200 nm in diameter and extend approximately 10 μm into the lumen of the nephron. Ciliary dysfunction is linked to autosomal dominant polycystic kidney disease, the most common of the inherited cystic diseases and thus, understanding the functioning of the cilium and the mechano-sensitive channels thereon is crucial to furthering research into the disease. The manner in which the cilium bends in response to fluid flow along the nephron and the mechanisms leading to the intracellular calcium release are widely debated. Here, an interdisciplinary approach has been adopted to investigate the biophysical properties of the primary cilium to gain insight into ciliary bending. Initially, fixed cells were imaged by Atomic Force Microscopy (AFM) in Intermittent Contact Mode (Figure 1) to confirm MDCK type II cells were manifesting primary cilia. On unfixed cell layers, a TCS SP5 Confocal Microscope (Leica, Wetzlar, Germany) was then used to identify cells with a primary cilium and then position the cantilever of the AFM instrument (JPK, Berlin, Germany) in the near vicinity of the cilium. We controllably probed individual primary cilia with the AFM cantilever tip with forces of up to 13.5 pN to obtain a vertical deflection map in one plane. By probing primary cilia at different heights from the surface of the cell, we produce AFM "deflection volume" data sets. This detailed probing of the mechanical response of the cilium as a function of height is a mechanical analogue of the z-stack optical imaging employed in confocal microscopy. Using this approach, we have measured the stiffness of the cilia, with spring constants of $4 \pm 2 \times 10^{-5} \text{ Nm}^{-1}$ (mean \pm S.E.M, $n=7$) consistent with other techniques (1, 2). This result supports the hypotheses of Schwartz et al. (1) and Resnick (2), in that the primary cilium bends due to mechanical strains of the order of 10^{-5} Nm^{-1} and hence is able to act as a flow sensor in the kidney.

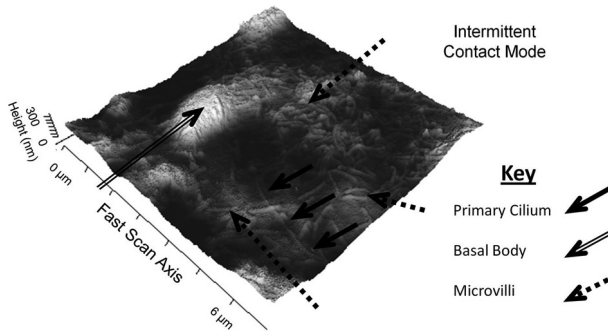


Figure 1: An AFM image of the apical surface of an MDCK Type II cell. Lighter colours indicate higher parts of the sample. A primary cilium (solid arrows) can be seen extending from the basal body (hollow arrow). The remaining hair-like structures on the surface are microvilli (dashed arrows).

Schwartz, E. A., et al., American Journal of Physiology-Renal Physiology 272 (1), F132 (1997).

Resnick, A., Journal of Biomedical Optics 15 (1), Article No.: 015005 (2010)

Funded by BBSRC, EPSRC and JPK Instruments (Berlin, Germany)

Where applicable, the authors confirm that the experiments described here conform with The Physiological Society ethical requirements.

C13 and PC13

The distribution of polycystic kidney disease channels in the organ of Corti

S. Mahendrasingam², R. Fettiplace³ and C.M. Hackney¹

¹Biomedical Science, University of Sheffield, Sheffield, Yorkshire, UK, ²Institute for Science and Technology in Medicine, Keele University, Stoke-on-Trent, Staffordshire, UK and ³Dept of Physiology, University of Wisconsin-Madison, Wisconsin, WI, USA

Polycystic kidney disease (PKD) channels, also known as TRPP channels, mediate the detection of fluid flow in cilia of renal epithelial cells and have characteristics in common with the mechanotransduction channels in inner ear hair cells. They are non-selective cation channels sensitive to extracellular calcium ion levels that have a large unitary conductance similar to the hair cell mechanotransduction channel (Fettiplace 2009). It is possible that one of the channel forming isoforms, PKD2, PKD2L and PKD2L1, have components in common with the hair cell mechanotransduction channel. Here we investigated the distribution of post-embedding immunogold labelling for the PKD2 component in the organ of Corti with respect to the sensory hair cells.

Rats were anaesthetised with an overdose of sodium pentobarbitone (0.8 ml/kg) according to individual weights. After complete loss of the pedal reflex (checked by toe pinch), they were decapitated and the cochleae excised. The cochleae and utri-

cles of four rats that could hear (P16 and P26) were perfused with 4% paraformaldehyde and 0.1% glutaraldehyde in sodium phosphate buffer (pH 7.4), immersion fixed in the same fixative and cochlear segments were dissected out in the same buffer. These were dehydrated through an alcohol series and embedded in LR White resin at a 50°C and labelled with an antibody to the PKD channels (Bethyl Labs, USA). Immunoblots of organ of Corti were performed with the antibody on tissue extracts from the cochleae of two rats that had undergone polyacrylamide gel electrophoresis and transferred to nitrocellulose sheets.

Immunoblotting showed a main band at 110 kDa, a molecular weight corresponding to the PKD2 protein. In the organ of Corti, labelling of the microtubules was also observed. These organelles transport proteins to sites where they are used by the cell so such transport recognition is a plausible hypothesis for this labelling. Labelling of stereociliary membranes was apparent in both inner and outer hair cells with some evidence of labelling towards the stereociliary tips. The membrane of the kinocilium in utricular hair bundles showed a similar density of labelling to their stereociliary membranes, so the stronger labelling of this organelle with immunofluorescence and confocal laser microscopy that has been reported by others may be accounted for by microtubular labelling.

We conclude that labelling for PKD2 is present in the stereocilia and the detection of PKD2 in the inner ear warrants more physiological investigation because there would be therapeutic benefits of determining further the characteristics of stereociliary ion channels.

Fettiplace R (2009). *Pflügers Arch* 458, 1115-1123.

Supported by a National Institute on Deafness and other Communicative Disorders grant RO1 DC 03896 and a Steenbock award to RF.

Where applicable, the authors confirm that the experiments described here conform with The Physiological Society ethical requirements.

C14 and PC14

The distribution of plasma membrane calcium ATPase 2 in stereociliary bundles of mammalian cochlear hair cells

J.A. Tickle¹, S. Mahendrasingam¹, C.M. Hackney², R. Fettiplace³ and D.N. Furness¹

¹*Institute for Science and Technology in Medicine, Keele University, Stoke-on-Trent, Staffordshire, UK,* ²*Biomedical Science, University of Sheffield, Sheffield, Derbyshire, UK* and ³*Physiology, University of Wisconsin-Madison, Madison, WI, USA*

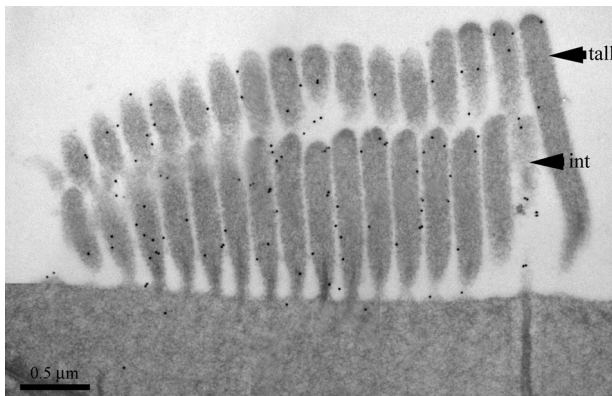
The predominant plasma membrane calcium ATPase (PMCA) within the stereociliary bundle of outer hair cells (OHC) of the mammalian cochlea is thought to be PMCA2s (Dumont et al, 2001). PMCA2a may be needed to regulate calcium in the bundle during mechanoelectrical transduction (MET), where calcium enters through the hair-cell MET channels. In rat OHC bundles there are three rows of stereocilia, short, intermediate and tall. Recently, it has been shown that MET channels are

located only in the short and intermediate rows of the three (Beurg et al., 2009) probably associated with the lower end of the tip link that emanates from the stereociliary tips. We hypothesised, therefore, that PMCA2a would be at higher concentration in the short and intermediate rows.

To test this hypothesis we performed post-embedding immunogold labelling on hair bundles from three regions of the rat cochlea. Two 26 day-old Sprague-Dawley rats were killed and the cochleae were removed and perfused with 4% p-formaldehyde and 0.1% glutaraldehyde in sodium phosphate buffer for 2 h, dissected, dehydrated and embedded in LR-White resin. Ultrathin sections of apical, middle and basal regions were cut and labelled with an antibody to PMCA2a and b isoforms (Abcam ab3529). The PMCA2b isoform is not thought to be expressed at high levels in the OHC. The primary antibodies were revealed by 10 or 15 nm gold-conjugated secondary antibodies.

PMCA2 labelling was concentrated along the stereociliary membrane (Fig. 1) in all three rows. By counting gold particles per unit membrane length, similar PMCA2 labelling densities were found in all three rows, with a slightly, but not significantly, lower density in the tallest row (ANOVA; $F = 2.019$ (2,323) $p > 0.05$). The PMCA2 labelling was present along the entire length of each stereocilium in each row, but most concentrated on the the shaft compared with the extreme tip or basal (ankle) region. The distributions were similar in all cochlear regions.

These results indicate that PMCA2 is found in all three rows of stereocilia with no evidence of an overall change in density corresponding to the presence or absence of the MET channels. This implies that PMCA2 is required not only to regulate calcium entering via the MET channel but also that which diffuses into the stereocilia from other cellular regions. There will also be a contribution to rapid calcium buffering by parvalbumin beta and calbindin D28K which are present in the stereocilia, although at lower concentration than in the cell body (Hackney et al 2005).



Ultrathin section of an immunogold labelled OHC bundle. Note the gold particles (black dots) tend to lie over the membrane of the stereocilia, and are present on the tallest (tall) and intermediate (int) rows. The short row is not represented in this image.

Beurg M et al (2009). *Nat. Neuroscience* **12**, 553-558.

Dumont RA *et al* (2001). *J Neurosci.* **21**, 5066-5078.

Hackney CM *et al* (2005). *J Neurosci.* **25**, 7867-7875.

Supported by the RNID (JT), The Steenbock Professorship (RF and SM) and the Henry Smith Charity (DNF).

Where applicable, the authors confirm that the experiments described here conform with The Physiological Society ethical requirements.

C15 and PC15

In lanceolate endings of rat hair follicles the small conductance Ca²⁺-activated K⁺ channel SK3 is found mainly in glial cells

F.C. Shenton¹, R.W. Banks¹ and G.S. Bewick²

¹*School of Biological & Biomedical Sciences, Durham University, Durham, UK and* ²*School of Medical Sciences, University of Aberdeen, Aberdeen, UK*

Autogenic modulation of mechanoreceptor excitability by Ca²⁺-dependent glutamate release from synaptic-like vesicles (SLVs) has been shown using the muscle spindle as a model (1). The excitability of lanceolate endings of hair follicles may be similarly regulated (2). In spindles Ca²⁺ entry through P/Q type channels activates KCa channels (BK or SK) to regulate afferent firing (3). In excitatory synapses of mouse hippocampus SK3 is a presynaptic channel (4) where it is probably involved in regulating neurotransmitter release. SK3 might therefore play a role in modulating glutamate release from SLVs. We have now studied SK3 expression in spindles and lanceolate endings, plus their associated satellite glial cells (SLGs) by immunocytochemistry. Synaptophysin (SYN, a marker of SLVs) was used to label sensory endings while the Ca²⁺-binding protein, S100 was used to identify SLGs.

Adult rats (2) were deeply anaesthetized with sodium pentobarbitone (45 mg kg⁻¹, I.P.) and fixed by transcardial perfusion (4% (w/v) paraformaldehyde in 0.1M phosphate buffer, pH 7.4; all procedures in accordance with ASPA 1986). Immunofluorescence labelling was carried out on 10 µm cryosections of pinna skin. Sections were double stained with one of four antibody combinations: 1) anti-SK3 (5 µg/ml, goat polyclonal Santa Cruz Biotechnology) + anti-SYN (1 µg/ml, mouse monoclonal Millipore); 2) anti-SK3 + anti-S100 (1:400, mouse monoclonal Santa Cruz Biotechnology); 3) anti-ASIC2 (5 µg/ml, goat polyclonal Santa Cruz Biotechnology) + anti-SYN; 4) anti-ASIC2 + anti-S100. Secondary antibodies were Alexa Fluor (AF) conjugated (AF 594 goat anti-rabbit and AF 488 goat anti-mouse, Invitrogen). Images were taken with a Leica SP5 Laser Scanning Microscope. Colocalisation of SK3 and ASIC2 reactivity with either S100 or SYN labelling was assessed by Pearson's correlation coefficient (r) using LAS AF Lite software (Leica Microsystems CMS GmbH).

We were unable to demonstrate SK3 in spindle terminals but it was present in the SLGs of lanceolate endings and, at lower levels, in the terminals themselves. Correlation of SK3 with S100 ($r = 0.34 \pm 0.05$, mean \pm SE) was greater than ASIC2 with S100 (0.15 ± 0.03), $P < 0.01$. SK3 correlation with SYN (0.24 ± 0.02) was less than

that of ASIC2 with SYN (0.42 ± 0.03), $P < 0.01$. SK3 correlation with S100 was greater than with SYN, but this did not reach statistical significance. Thus, SK3 was expressed predominantly in SLGs. By contrast immunolabelling for the Na⁺ ion channel ASIC2, previously reported in lanceolate endings (5) and SYN were largely coincident. Our data suggest that in lanceolate endings SK3 is expressed predominantly in SLG's. SK3 channels could play a role in shaping SLG responses to fluctuations in intracellular Ca²⁺ and thereby indirectly influence afferent excitability of the terminals.

- 1) Bewick, G.S., B. Reid, et al. (2005). Autogenic modulation of mechanoreceptor excitability by glutamate release from synaptic-like vesicles: evidence from the rat muscle spindle primary sensory ending. *Journal of Physiology-London* 562(2): 381-394.
- 2) Shenton, F.C., H. Wollner, et al. (2009). Immunogold labelling for glutamate in lanceolate endings of mouse hairs. Oral presentation Physiol. Soc. Cellular & Integrative Neuroscience Themed Meeting, Cardiff, UK
- 3) Simon, A., R. W. Banks et al. (2009). P/Q type Ca²⁺ & KCa channel blockers increase afferent discharge from mechanosensory terminals. Oral presentation Physiol. Soc. Cellular & Integrative Neuroscience Themed Meeting, Cardiff, UK
- 4) Obermair, G. J., W. A. Kaufmann, et al. (2003). The small conductance Ca²⁺-activated K⁺ channel SK3 is localized in nerve terminals of excitatory synapses of cultured mouse hippocampal neurons. *European Journal of Neuroscience* 17(4): 721-731.
- 5) Price, M. P., G. R. Lewin, et al. (2000). The mammalian sodium channel BNC1 is required for normal touch sensation. *Nature* 407(6807): 1007-1011.

Where applicable, the authors confirm that the experiments described here conform with The Physiological Society ethical requirements.

C16 and PC16

Heritability of mechanosensory traits in humans

H. Frenzel¹, J. Bohlender², K. Pinsker², M. Gross² and G.R. Lewin¹

¹Department of Neuroscience, Max-Delbrück-Center for Molecular Medicine (MDC) Berlin-Buch, Berlin, Germany and ²Clinic for Audiology and Phoniatrics, Charité - Universitätsmedizin Berlin, Berlin, Germany

The aim of this study was to explore the genetics of different sensory traits in humans with a focus on traits that rely on the transduction of mechanical stimuli. In a classical twin study, the heritability of the different traits was determined. One hundred twin pairs participated in the study, of which 66 were monozygotic and 34 were dizygotic. Heritability values were estimated by structural equation modeling (1). Two aspects of touch sensitivity were investigated, the vibration detection threshold and tactile acuity. For vibration detection threshold determination, a sinusoidal 125 Hz vibration was applied proximal to the nail of the little finger and the detection threshold determined as an amplitude. For the vibration detection threshold a very robust heritability value of 0.52 (0.33 – 0.67, 95 % confidence interval (CI)) was estimated. In the tactile acuity test, the ability to detect the orientation of gratings of different spacing with the fingertip of the little and index fingers was assessed and a thresh-

old in mm determined. The estimated heritability value was 0.27 (0.05 – 0.46 95 % CI). This is the first report about a genetic contribution to the variation of touch sensitivity in humans. Three parameters of hearing were investigated, the pure tone threshold in decibel (dB) and the strength as well as the reproducibility of the otoacoustic emissions, the latter two being measures of outer hair cell function. The heritability estimates for all three measures were very high at 0.80 (0.67 – 0.87, 95 % CI), 0.76 (0.62 – 0.85, 95 % CI) and 0.88 (0.80 – 0.93, 95 % CI), respectively. A third mechanosensory system was tested, the vascular baroreflex, a system that senses and balances short term changes in blood pressure. Baroreflex slope, a measure of the strength of reflex reactions showed a heritability value of 0.39 (0.17 – 0.57, 95 % CI) and estimated heritability of baroreflex sequence frequency, which is the number of baroreflex reactions in a certain period of time at rest, was 0.56 (0.34 – 0.71, 95 % CI). We found significant correlation between some of these mechanosensory traits on a phenotypic level, e.g. between tactile acuity and pure tone thresholds ($r = 0.16$; $p < 0.05$, t-test). One of the investigated systems does not require transduction of mechanical stimuli, the cutaneous thermosensory system. We could determine values for the heritability of cold and warmth detection thresholds, 0.40 (0.16 – 0.60, 95 % CI) and 0.37 (0.14 – 0.56, 95 % CI), respectively. In contrast, we did not find a significant heritability of heat and cold-pain thresholds. These results show that most of the investigated traits and all of the mechanosensory traits show significant heritability. Genetic influences on these traits are thus assessable by routinely used medical testing equipment. We demonstrated the usability of the employed tests for use in genome-wide approaches.

Neale MC, Maes HHM: Methodology for genetic studies of twins and families; Dordrecht, Netherlands; Kluwer Academic Publishers; 2004.

Supported by the DFG (SFB 665).

Where applicable, the authors confirm that the experiments described here conform with The Physiological Society ethical requirements.

C17 and PC17

The mechanics of the tympanal ear of locust

T. McDonagh^{1,2}, J. Windmill^{1,3} and D. Robert¹

¹School of Biological Sciences, University of Bristol, Bristol, Avon, UK, ²Laboratory of Sensory Neuroscience, The Rockefeller University, New York, NY, USA and ³Department of Electronic and Electrical Engineering, University of Strathclyde, Glasgow, UK

In the ear of the locust (*S.gregaria* Forskål), frequency analysis arises from the mechanical properties of the tympanal membrane¹. Incident sound is spatially decomposed into discrete frequency components through a tympanal traveling wave that localizes mechanical energy to specific tympanal locations, where distinct groups of mechanoreceptor neurons project². To understand the exact mechanics of the tympanal traveling wave, its motion was measured by scanning laser vibrom-

etry to characterize its response to short frequency stimuli, with a resolution of 390 ns. This allows the measurement of the instantaneous wave velocity and the direct observation of a wave compression across the tympanum. A thin region on the tympanal membrane's posterior edge is the collection area for acoustic energy. The apparent function of the subsequent converging traveling waves is to localize kinetic energy from $\sim 2 \text{ nJ/m}^2$ at the start of the traveling waves, to $\sim 12 \text{ nJ/m}^2$ where it terminates at the mechanoreceptor neuron projections. Traveling wave velocities were compared with two competing model of mechanics: the thin-film and stiff-plate models. Wave velocity was found to have limited frequency dependence, thus suggesting that stiffness was not a dominant property of the membrane's mechanics. Therefore, although the locust tympanal membrane exhibits a similar phenomenon to the traveling wave of von Békésy on the mammalian basilar membrane³, it appears that the locust traveling wave is not produced by a stiffness gradient, such as that which causes the von Békésy basilar membrane traveling wave.

Windmill J et al. (2005). *J Exp Biol* 208 (1), 157-168

Jacobs K et al. (1999). *J Exp Zool* 283, 270–285

von Békésy, G. (1960). *Experiments in Hearing*. New York: McGraw-Hill.

This work was supported by the Biotechnology and Biological Science Research Council (UK), and the UK-IRC in Nanotechnology.

Where applicable, the authors confirm that the experiments described here conform with The Physiological Society ethical requirements.

C18 and PC18

Glucocorticoids cause only a transient increase in the surface abundance of the epithelial Na⁺ channel (ENaC) subunits (α -, β - and γ -ENaC) in H441 human airway epithelial cells

N. Ismail, S.C. Land and S.M. Wilson

Centre of Cardiovascular and Lung Biology, University of Dundee, Dundee, UK

Glucocorticoids control epithelial Na⁺ conductance via a mechanism dependent upon serum and glucocorticoid-inducible kinase 1 (SGK1) a kinase thought to control the surface abundance of α -, β - and γ -ENaC. However, whilst dexamethasone activates SGK1 in H441 cells, this response is rapid (1 – 3 h) and transient whilst the induction of Na⁺ current is relatively slow (> 3 h) and sustained (Watt et al. 2010). We have therefore explored the effects of dexamethasone upon α -, β - and γ -ENaC abundance in the total and in surface protein pools; surface proteins were isolated by biotinylation (10mM sulfo succinimidyl-2-(biotinamido)-ethyl-1,3'-dithiopropionate, 1 h 4°C) / streptavidin binding.

Two α -ENaC isoforms ($\sim 100 \text{ kDa}$ and $\sim 77 \text{ kDa}$) were detected in total and surface pools and dexamethasone (0.2 μM , 24 h) consistently increased the abundance of each isoform in both protein pools (Fig. 1A). Beta-ENaC was present as a single band

(~100 kDa) and, whilst dexamethasone clearly increased the overall expression of this subunit, it had no effect upon surface abundance. Although two γ -ENaC isoforms (96 kDa, 76 kDa) were detected in total protein, only one band (~80 kDa) was present at the cell surface and dexamethasone had no effect upon the abundance of this surface-exposed protein (Fig. 1A). Each ENaC subunits is therefore present at the surface of glucocorticoid-deprived cells, and the fact that such cells do not display Na^+ currents (Watt et al. 2010) cannot, therefore, be attributed to the absence of α -, β - and γ -ENaC from the membrane. Moreover, the induction of ENaC activity by prolonged (~24 h) dexamethasone stimulation is not associated with any change to the surface expression of β - and γ -ENaC whilst the effect on α -ENaC can be explained by an increase in the overall expression level (Fig1 A).

Since glucocorticoid-induced SGK1 activity peaks after ~3 h (Watt et al. 2010), subsequent experiments compared the abundance of α -, β - and γ -ENaC at the surface of hormone-deprived cells, and cells exposed to 0.2 μM dexamethasone for 24 h or 3h. As anticipated (see above) 24 h stimulation increased the surface expression of α -ENaC with no effect upon β - or γ -ENaC (Fig. 1B). Increases in the surface abundance of α -, β - and γ -ENaC were, however, evident in cells exposed to dexamethasone for only 3 h (Fig. 1B), despite the fact that such cells do not express discernible Na^+ currents (Watt et al. 2010).

Whilst periods of SGK1 activation are associated with the recruitment of α -, β - and γ -ENaC to the cell surface, such co-ordinated increases in the surface expression of these channel subunits cannot explain the SGK1-dependent activation of ENaC in these cells (Watt et al. 2010).

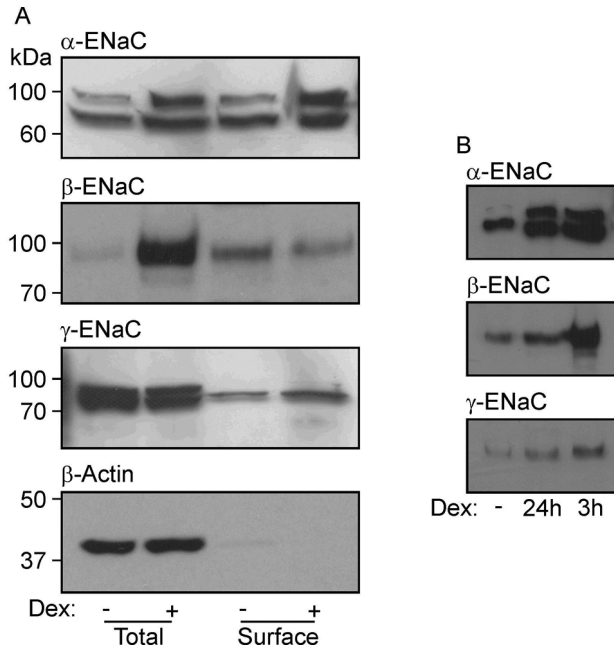


Figure 1. (A) Western blots showing the abundances of α -, β - and γ -ENaC and β -actin in total and surface-exposed proteins extracted from cells that had maintained (24 h) in hormone-free medium or in medium containing $0.2 \mu\text{M}$ dexamethasone. The lack of β -actin from the surface pool confirms that this protein preparation is essentially devoid of intracellular proteins. Essentially identical results were obtained in 5 experiments. (B) Abundances of α -, β - and γ -ENaC in surface exposed proteins isolated from glucocorticoid-deprived cells and from cells at identical passage that had been exposed to $0.2 \mu\text{M}$ dexamethasone for 3 h or 24 h ($n = 3$).

Watt GB, Land SC & Wilson SM (2010). *Proc. Physiol. Soc.* this meeting.

Supported by a grant from the Wellcome Trust and studentship from the Government of Malaysia (NASI).

Where applicable, the authors confirm that the experiments described here conform with The Physiological Society ethical requirements.

PC19

Neurokinin B suppresses gonadotrophin-releasing hormone pulse generator frequency in female rats

P. Grachev, J.S. Kinsey-Jones, X.F. Li and K.T. O'Byrne

Division of Women's Health, King's College London, London, UK

Neurokinin B (NKB) and its G protein-coupled receptor (NK3-R) are essential for physiologic gonadotrophin secretion, reproductive development and fertility. NKB/NK3-R neurones are particularly numerous in the hypothalamic arcuate (ARC) nucleus, which is known to be the site of the gonadotropin-releasing hormone (GnRH) pulse generator. The purpose of this study was to determine whether manipulation of NKB/NK3-R signalling in the ARC impacts on endocrine and electrophysiological manifestations of the GnRH pulse generator frequency. We examined the effect of a selective NK3-R agonist, Senktide – administered intra-ARC – on pulsatile luteinizing hormone (LH) secretion in the rat. Adult female rats were anaesthetised using ketamine (100 mg/kg, i.p.) and xylazine (10 mg/kg, i.p.), bilaterally ovariectomised and implanted with subcutaneous 17 β -oestradiol (E2) capsules (which produce circulating concentrations of E2 within the range observed during the diestrus phase of the estrous cycle, 38.8 ± 1.2 pg/ml). These were then chronically implanted with bilateral intra-ARC cannulae and intravenous catheters. Blood samples (25 μ l) for LH measurement were automatically collected from the freely moving animals every 5 min for 6 h using a custom-built automated serial blood sampling system. After 2 h of control blood sampling, Senktide (1-10 pmol in 400 nl total injected volume, bilaterally; n = 14), or artificial cerebrospinal fluid (aCSF) vehicle (n = 5) was administered via the pre-implanted cannulae. Senktide significantly ($p < 0.005$; 2-tailed paired Student's T-test) abolished LH pulses immediately following intranuclear administration. The duration of Senktide-dependent LH pulse inhibition was dose-dependent (90-200 min) with subsequent recovery of normal LH pulse frequency. To confirm that this effect was due to altered firing of neurones in the ARC, the hypothesised site of the GnRH pulse generator, we used electrophysiological techniques to record multiple-unit activity (MUA) in this region of the hypothalamus. MUA volleys correlate invariably with LH pulses, and are thus a reliable electrophysiological correlate of GnRH pulse generator activity. Ovariectomised rats (n = 5) were chronically implanted with intra-ARC electrode assemblies comprising 9 electrodes and intracerebroventricular (i.c.v.) cannulae aimed at the lateral ventricle. Following the detection of a basal MUA volley frequency, a range of doses of Senktide (100-600 pmol in 4 μ l aCSF) was administered via pre-implanted cannulae. Senktide caused significant ($p < 0.005$; 2-tailed paired Student's T-test) suppression of MUA volleys lasting 90-130 min. MUA volley frequency gradually returned to baseline following the suppression. These data suggest that NKB might act at the level of the hypothalamic ARC nucleus to suppress GnRH pulse generator frequency.

P.G. - KCL Graduate School PhD Studentship

Where applicable, the authors confirm that the experiments described here conform with The Physiological Society ethical requirements.

PC20

FK506-binding proteins regulate SOCE in human platelets by calcineurin-dependent and -independent pathways

E. López, G.M. Salido, J.A. Rosado and P.C. Redondo

Physiology, University of Extremadura, Cáceres, Extremadura, Spain

FK506 binds to the members of the FK506-binding protein (FKBP) subfamily of immunophilins inhibiting their peptidyl-prolyl isomerase (PPI) activity, which has been shown to be required to modulate the permeability of endoplasmic reticulum-resident calcium channels, like IP₃R and RYR (Adams et al., 2005; Kumar et al., 2005; MacMillan et al., 2008). Here we investigate the role of FKBP during the activation of SOCE in human platelets.

Human platelets were obtained from healthy volunteers according to the Declaration of Helsinki as previously described (Rosado and Sage, 2000). Incubation of fura 2-loaded platelets with FK506 for 5 min modified calcium release from intracellular pools and SOCE in human platelets. Low FK506 concentrations (up to 10 μ M) increased SOCE activation induced either with thapsigargin (TG, 200 nM) or thrombin (Thr, 0.1 U/ml), meanwhile higher FK506 concentrations (50 μ M) significantly reduced SOCE ($P < 0.05$; Student's t test). Platelets incubation with 2-APB (100 μ M) for 30 min at 37°C attenuated the increased calcium release evoked by FK506; although an alternative mechanism of calcium release sensible to FK506 in human platelets still remained active.

Human platelets incubation for 30 min with the calcineurin (CNa) antagonist cyclosporin A (100 nM; MacMillan et al., 2008) or for 5 min with cyclosporin A (50 μ M; Adams et al., 2005) reduced TG-evoked SOCE, which indicates that CNa activity is required for the activation of SOCE. Furthermore, inhibition of FKBP's PPI activity by incubation for 30 min with rapamycin (500 nM), which does not affect CNa activity, also reduced significantly TG-induced SOCE.

Co-immunoprecipitation experiments revealed that FK506 reduced Thr- and TG-induced IP₃R II/TRPC1 coupling, which plays an important role in the maintenance of SOCE. The association between TRPC1 and FKBP12 was sensitive to FK506 and rapamycin. In contrast, the coupling of TRPC1 with CNa was affected by FK506 but insensitive to rapamycin.

In summary, here we show for the first time that the activity of the immunophilin subfamily FKBP is important for the activation of SOCE by both CNa-dependent and -independent pathways in human platelets.

Adams B et al. (2005). *J Biol Chem* 280, 24308-14.

Kumar R et al. (2005) *Mol Biochem Parasitol* 141, 163-73.

MacMillan D et al. (2008) *Cell calcium* 43, 539-49.

Rosado JA & Sage SO (2000) *J Biol Chem* 276, 15659-65.

This work is supported by MEC (BFU2010-21043-C02-01), AECID-PCI (A/023417/09) and Fundesalud (PRI090046). Redondo PC is supported by RYC program (RYC-20070-00349) and Lopez E is supported by Carlos III health programm (FI10/00573).

Where applicable, the authors confirm that the experiments described here conform with The Physiological Society ethical requirements.

PC21

Induction of aromatase expression and activity and steroid receptors expression in endometriotic cells: effects of oxidative stress and estradiol

L. Noordin¹, T. Rizner² and E.M. Ellis³

¹SIPBS, University of Strathclyde, Glasgow, UK, ²Institute of Biochemistry, Faculty of Medicine, University of Ljubljana, Ljubljana, Slovenia and ³SIPBS, University of Strathclyde, Glasgow, UK

Endometriosis is a complex gynaecological disease characterized by ectopic endometrial tissue outside of the uterus. Several factors have been reported to promote endometriotic cell proliferation. We have shown previously that oxidants and the lipid peroxidation product acrolein can significantly induce endometriotic cell proliferation, and this proliferation is aggravated by estradiol. To date, the precise molecular mechanism by which estrogens act on endometriotic cell proliferation remains obscure. The aims of this study are i) to investigate factors that affect the expression of aromatase (CYP19) and steroid hormone receptors (estradiol and progesterone) and ii) to determine the expression of aromatase (CYP19) in human samples of normal endometrium and from ovarian endometriosis.

Immortalized human endometriotic epithelial cells (12-z) (obtained with consent from patients undergoing surgery) were treated with estradiol (10^{-8} M) alone for 24 hours or in combination with the oxidants H_2O_2 (1 μ M) or menadione (20 μ M), or the lipid peroxidation product acrolein (20 μ M) for 48 hours. The expression of aromatase in 12-z cells was determined by Western blotting and aromatase activity was determined using an estrone ELISA. The expression and activity of aromatase was found to be significantly higher in 12-z cells treated with oxidants, lipid peroxidation products and estradiol as compared to untreated control. In addition, the expression of aromatase in ovarian endometriosis was significantly higher than in normal endometrium. This suggests that this enzyme may contribute to cell proliferation as aromatase is a key enzyme of local estradiol production.

The expression and localization of estradiol- α (ER- α), estradiol- β (ER- β) and progesterone (PR) receptors were determined by Quantitative Reverse Transcriptase-Polymerase Chain Reaction (Q-RT-PCR) and Western blotting. A significant upregulation of ER- α expression was observed in cells treated with oxidants, lipid peroxidation products and estradiol, particularly with the combination of oxi-

dants/acrolein and estradiol. No increase in ER- β and PR expression was observed, indicating that they are not involved in the response to oxidants and estradiol. In summary, changes in gene expression by oxidants and estradiol mimics the physiological situation in endometriosis and provides potential areas for therapeutic intervention.

Where applicable, the authors confirm that the experiments described here conform with The Physiological Society ethical requirements.

PC22

Comparison of gadolinium and FM1-43 as blockers of stretch-evoked firing of rat muscle spindle afferents

S. Watson¹, C. Aryiku¹, R.W. Banks² and G.S. Bewick¹

¹School of Medical Sciences, University of Aberdeen, Aberdeen, UK and ²School of Biological & Biomedical Sciences, University of Durham, Durham, UK

The identity and properties of the mechanotransduction channel within muscle spindles, the proprioceptive sensory organs reporting skeletal muscle length, are poorly understood. We have shown previously that stretch releases glutamate from synaptic-like vesicles (SLVs) within the spindle terminals, activating an unusual metabotropic glutamate receptor (mGluR) linked to phospholipase D and increasing afferent firing (Bewick *et al*, 2005). However, the stretch activated channel(s) causing the initial depolarization and triggering SLV fusion with the membrane remains unidentified. To further characterise these channels we tested the effects of gadolinium (Gd^{3+}), a lanthanoid, and FM1-43, a styryl pyridinium dye, which both block electrical currents mediated through stretch-activated channels in other systems (Yang & Sachs, 1989; Hajduczuk *et al*, 1994; Gale *et al*, 2001; Drew & Wood, 2007). Adult male Sprague-Dawley rats (360-430 gm) were humanely killed then 4th lumbrical nerve-muscle preparations excised and equilibrated under gassed (95%O₂-5%CO₂) saline. Spindle discharges were recorded en passant from the muscle nerve with Ag⁺ wire electrodes at room temperature during 1 mm stretch-and-hold cycles (~10% muscle length). The effect of increasing concentrations of Gd^{3+} and FM1-43 applied for at least 60 min on stretch-evoked firing was compared to responses in saline alone. Differences in mean firing frequencies (impulses per second, imp/sec) between the drug-free and in-drug conditions were evaluated by paired *t*-test or one way ANOVA followed by Tukey multiple comparison post-tests, as appropriate, with a significance threshold of $P = 0.05$. 100 μM Gd^{3+} decreased firing from 353.4 ± 23.6 to 272.3 ± 16.2 imp/sec (mean \pm SE; $n = 6$, $P < 0.01$) after 1 hr incubation. 1 mM Gd^{3+} did not decrease the firing rate further but 10 mM abolished firing altogether ($P < 0.0001$). Some firing returned after 1 hr wash. However, the firing rates (29.4 ± 12.0 imp/sec) were well below pre-treatment rates. In contrast, 5 μM FM1-43 had no significant effect on firing (from 267.1 ± 6.8 to 286.9 ± 12.5 imp/sec, $n = 3$; $P = 0.41$ at 3 hr). At 10 μM , the dye decreased firing by ~30% (to 152.8

± 39.5 imp/sec; $P < 0.01$) after 3 hrs, a concentration producing $\sim 80\%$ block of currents in cultured sensory neurones (Drew *et al.*, 2007). Dye does penetrate the selectively permeable spindle capsule under these conditions, as $5 \mu\text{M}$ FM1-43 labels these terminals in only 2 hr (Bewick *et al.*, 2005). These data indicate that stretch-activated channels that initiate stretch-activated afferent discharges in muscle spindles are Gd^{3+} sensitive but relatively insensitive to FM1-43.

Bewick GS, *et al.* (2005). *J Physiol* 562, 381-394.

Drew L & Wood J (2007). *Molecular Pain* 3, 1.

Gale JE, *et al.* (2001). *J Neurosci* 21, 7013-7025.

Hajduczuk G, *et al.* (1994). *J Clin Invest* 94, 2392-2396.

Yang XC & Sachs F (1989). *Science* 243, 1068-1071.

This work was supported by a SULSA collaborative BioScape grant with Eli Lilly Corp (SW) and a Nuffield Undergraduate Bursary (C-LA).

Where applicable, the authors confirm that the experiments described here conform with The Physiological Society ethical requirements.

PC23

Glucocorticoid-induced activation of epithelial Na^+ channels (ENaC) in H441 human airway epithelial cells does not coincide with increased activity of serum and glucocorticoid regulated kinase 1 (SGK1)

G.B. Watt, S.C. Land and S.M. Wilson

Centre for Cardiovascular and Lung Biology, University of Dundee, Dundee, UK

Airway function is dependent upon the absorption of Na^+ from the airway surface liquid and this ENaC-dependent process is regulated by glucocorticoids. These hormones induce expression SGK1 (see e.g. Cohen & Lang, 2001), a regulatory kinase that seems to stimulate Na^+ transport by increasing the surface abundance of ENaC subunits. The catalytic activity of SGK1 is dependent upon the phosphoinositide-3-kinase (PI3K)-controlled phosphorylation of SGK1-Ser⁴²² by the mammalian target of rapamycin signalling complex 2 (TORC2) (García-Martínez & Alessi, 2008) and, to clarify the mechanism that allows glucocorticoids to control ENaC, we now explore the effects of inhibitors of TORC2 (TORIN1) and SGK1 (GSK650394) upon the glucocorticoid-induced epithelial Na^+ current (Clunes *et al.*, 2004) and SGK1 activity (assayed by monitoring the phosphorylation of NDRG1-Thr^{346/356/366}, an endogenous SGK1 substrate, see Inglis *et al.* 1999) in H441 cells.

Initial studies confirmed (see Clunes *et al.*, 2004) that ~ 24 h exposure to $0.2 \mu\text{M}$ dexamethasone depolarizes V_m (Fig 1A) by inducing amiloride-sensitive Na^+ current (Fig. 1B). This glucocorticoid-induced current was abolished by TORIN1 (Fig. 1C) or GSK650394 (Fig 1D). Although TORIN1 inhibits TORC1 as well as TORC2, this cannot explain the present effect since rapamycin, a selective TORC1 inhibitor, had no effect (Fig. 1E). Analyses of extracted proteins ($n = 4$) showed that TORIN1 ($0.1 \mu\text{M}$,

3 h) and GSK650394 (10 μ M, 3 h), but not rapamycin (0.1 μ M, 3 h), also blocked NDRG1-Thr^{346/356/366} phosphorylation indicating inactivation of this kinase. These compounds did not, however, suppress the PI3K-dependent phosphorylation of protein kinase B-Thr³⁰⁸ demonstrating that PI3K activity is retained. Glucocorticoid-induced ENaC activity in H441 cells is therefore dependent upon TORC2 / SGK1 but, despite this finding, subsequent studies showed that dexamethasone (0.2 μ M, ~24 h, n = 5) did not stimulate NDRG1-Thr^{346/356/366} phosphorylation. Moreover, whilst increased phosphorylation of this SGK1 substrate was evident in cells exposed to dexamethasone 3 h, brief (3 – 4 h) exposure to dexamethasone did not alter the electrical properties of H441 cells (n = 5). The glucocorticoid-induced Na⁺ currents in these cells thus develop relatively slowly but are maintained whilst SGK1 activation is more rapid and transient. It is therefore clear that hormone-induced ENaC activation does not coincide with the increased activity of SGK1 and so, whilst SGK1 is clearly important, our data suggest that the role of this kinase is permissive.

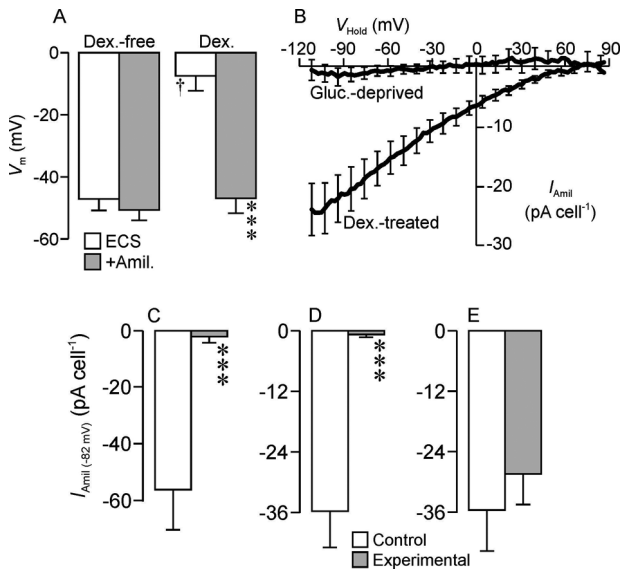


Figure 1. Membrane currents evoked by ramp changes in holding potential (V_{Hold}) were recorded in the perforated patch configuration during exposure to standard extracellular saline (ECS) and during exposure to 10 μ M amiloride (+Amil). (A) Effects of amiloride upon V_m in glucocorticoid-deprived and dexamethasone-treated (0.2 μ M, ~24 h) cells. (B) Effects of dexamethasone (0.2 μ M, ~24 h) upon the amiloride-sensitive component of the membrane current (I_{Amil}). The amiloride sensitive current flowing at -82 mV ($I_{Amil}(-82 mV)$) was quantified in dexamethasone-treated (0.2 μ M, ~24 h) control cells and in cells exposed (3 h) to 0.1 μ M TORIN1 (C), 10 μ M GSK650394 (D) or 0.1 μ M rapamycin (E). All data are mean \pm s.e.m and $n > 4$. Asterisks denote significant differences between control and experimental data ($P < 0.001$, Student's paired t test), the dagger denotes a statistically significant effect of dexamethasone ($P < 0.05$, ANOVA).

Clunes MT et al. (2004). *J. Physiol.* **557**, 809-819.

García-Martínez JM & Alessi DR. (2008). *Biochem. J.* **416**, 375-385.

Lang F & Cohen P. (2001). *Science STKE* **108**, RE17.

Inglis SK *et al.* (2009). *Pflügers Arch.* **457**, 1287-1301.

Supported by grants from the Wellcome Trust and a Studentship from the John George and Sheilah Livanos Charitable Trust (GBW).

Where applicable, the authors confirm that the experiments described here conform with The Physiological Society ethical requirements.

PC24

Effects of the cold pressor test on normotensive and hypertensive Nigerians before and after salt-loading

S.O. Elias^{1,2}, G.A. Umoren¹, S.I. Jaja² and O.A. Sofola²

¹Physiology, Lagos State University College of Medicine, Ikeja, Lagos, Lagos State, Nigeria and ²Physiology, College of Medicine of the University of Lagos, Lagos, Lagos, Nigeria

BACKGROUND: Blood pressure hyper-reactors are individuals who respond with an increase in systolic blood pressure (Δ SBP) and/or diastolic blood pressure (Δ DBP) of ≥ 15 mmHg to the cold pressor test(1). Hyper-reactivity is considered to be a useful indicator of future hypertension in normotensive individuals (2).

AIM: This study was designed to determine the effects of the cold pressor test (CPT) on the cardiovascular status of normotensive and hypertensive Nigerians before and after salt-loading.

METHODS: Normotensive (n=38) and hypertensive (n=45) subjects were exposed to the CPT by foot immersion in cold slurry at 4°C for 1 minute(3) after control parameters had been recorded. Vascular reactivity was then determined using the parameters described earlier(1). Thereafter, salt-loading was carried out with 200mmol/day of Na⁺ as sodium chloride for 5 days after which tests of blood pressure reactivity were repeated. Data were analysed using paired and unpaired Student t tests as appropriate. Data are presented as mean \pm S.E.M. and differences between means accepted as significant at 95% confidence level.

RESULTS: In normotensive subjects, systolic and diastolic blood pressures rose from 117.8 \pm 1.6 mmHg to 132.7 \pm 2.7 mmHg (p<0.0001) and 79.7 \pm 0.9 mmHg to 93.58 \pm 1.8 mmHg (p<0.0001) respectively after CPT. In hypertensive subjects, systolic and diastolic blood pressures rose from 143.8 \pm 2.9 mmHg to 162.9 \pm 3.5 mmHg (p<0.0001) and from 95.78 \pm 1.6 mmHg to 110.8 \pm 1.9 mmHg (p<0.0001) respectively. Before salt-loading, 44.7% of the normotensive subjects demonstrated systolic hyper-reactivity and 39.5% showed diastolic hyper-reactivity while among the hypertensive subjects, 51.0% and 36.8% demonstrated systolic and diastolic hyper-reactivity respectively before salt-loading. Systolic hyper-reactivity increased to 68.4% in normotensive subjects while 36.8% showed diastolic hyper-reactivity following salt-

loading. In hypertensive subjects, systolic and diastolic hyper-reactivity fell to 44.4% and 37.8% respectively following salt-loading.

DISCUSSION: Systolic BP response to the CPT is more consistent than diastolic reactivity in both normotensive and hypertensive subjects. Since vascular hyper-reactivity usually precedes sustained hypertension, it is possible that enhanced vascular reactivity plays an important role in the aetiology of hypertension among Nigerians.

Moriyama K, Ifuku H. (2010). *Eur J Appl Physiol* 108: 837-43

Siegrist PT, Gaemperli O, Koepfli P. et al (2006). *J Nucl Med* 47:1420-1426

Rubenfire M, Rajagopalan S, Mosca L (2000). *J Am Coll Cardiol* 36P 2192-2197

Where applicable, the authors confirm that the experiments described here conform with The Physiological Society ethical requirements.

PC25

Contraction-driven skeletal muscle differentiation in the embryo

R. Ashworth¹, U. Karunarathna¹, M. Lahne² and C. Krivcevska¹

¹*School of Biological and Chemical Sciences, Queen Mary University of London, London, UK and* ²*Galvin Life Science Building, University of Notre Dame, Notre Dame, IN 46556, IN, USA*

Contraction drives not only movement but skeletal muscle differentiation within the embryo. Establishing muscle structure during development is critical for later function; however, the steps that connect contraction to differentiation remain unclear. Using the zebrafish (*Danio rerio*), we revealed that myofibril organization within the developing skeletal muscle is dependent on the excitation-contraction (E-C) pathway, namely actin-myosin interaction [1, 2]. Our current work is aimed at identifying the signaling components that control muscle differentiation. In mature muscle, adhesion complexes form an important route for force transmission between the extracellular matrix and the cytoskeleton. Focal adhesion kinase (FAK) is a component of the adhesion complex and its activity regulates mechanotransduction. In the zebrafish embryo FAK phosphorylation coincides with somite formation and may play a role in skeletal muscle morphogenesis [3]. The action of FAK in embryonic skeletal muscle was assessed by treating embryos with inhibitors and examining the developmental consequences. Inhibitor 14 (Tocris) decreases FAK phosphorylation at tyrosine 397 (Tyr³⁹⁷), an autophosphorylation site that is critical for downstream signaling. Wild type zebrafish embryos were exposed to Inhibitor 14 (50 μ M – 1mM) for 6 hrs starting at 18 hpf, a time that coincides with the initiation of embryonic movement. Drug treatment at 500 μ M and 1mM resulted in significant abnormalities and death, whereas development at the lower concentrations appeared normal. Inhibitor 14 treated (50-250 μ M) and control embryos were fixed at 24 hpf and the myofibril structure and somite boundary formation analysed by immunocytochemistry using primary antibodies that recognise myosin and β -dys-

troglycan respectively. No differences in myofibril organisation or somite boundary formation between control and drug treated embryos were observed. Experiments were repeated with Okadaic acid (OA, Tocris), a phosphatase inhibitor reported to cause a loss of focal adhesions and dephosphorylation of FAK on Tyr³⁹⁷. OA drug uptake was facilitated by performing tail-cuts on the embryos and treatment (0.5 μ M and 1 μ M) appeared to cause a decrease in embryonic movements (tail-flipping and response to touch). However, there were no obvious defects in myofibril structure and somite boundary formation, as assessed by immunocytochemistry. In summary, application of FAK inhibitors to early embryos does not appear to disrupt skeletal muscle development, further work to determine the extent of FAK phosphorylation in the inhibitor-treated embryo will be necessary to confirm these initial observations. The mechanosensitive components of the contraction-driven skeletal muscle differentiation pathway *in vivo* remain to be established.

1. Brennan, C., Mangoli, M., Dyer, C.E., and Ashworth, R. (2005). Acetylcholine and calcium signalling regulates muscle fibre formation in the zebrafish embryo. *J Cell Sci* 118, 5181-5190.

Lahne, M., and Ashworth, R. (2009). A Contraction-dependent Pathway Regulates Myofibril Organization during Skeletal Muscle Development *in vivo*. *Journal of General Physiology* 134 17A.

Crawford, B.D., Henry, C.A., Clason, T.A., Becker, A.L., and Hille, M.B. (2003). Activity and distribution of paxillin, focal adhesion kinase, and cadherin indicate cooperative roles during zebrafish morphogenesis. *Mol Biol Cell* 14, 3065-3081.

This work was funded in part through a Physiological Society Vacation studentship to U. Karunarathna.

Where applicable, the authors confirm that the experiments described here conform with The Physiological Society ethical requirements.

PC26

STIM1 is expressed in acidic Ca²⁺ stores in human platelets and associates with Orai1 and TRPC channels upon Ca²⁺ store depletion

N. Dionisio, H. Zbidi, I. Jardín, G.M. Salido, P.C. Redondo and J.A. Rosado

Department of Physiology, Cell Physiology Research Group, University of Extremadura, Cáceres 10071, Spain

Cells accumulate Ca²⁺ into agonist-sensitive acidic organelles, such as secretory granules and lysosome-related organelles, which express a vacuolar proton-ATPase (V-ATPase) responsible for the maintenance of a proton gradient across their membranes. Current evidence suggests that, in human platelets, acidic Ca²⁺ stores are involved in the activation of store-operated Ca²⁺ entry (SOCE) (Rosado *et al.*, 2004), a mechanism for Ca²⁺ influx controlled by the filling state of the Ca²⁺ stores. Although STIM1 is considered the endoplasmic reticulum Ca²⁺ sensor, its presence and sensing role in the acidic stores have not been studied yet. Here we have investigated

the expression of STIM1 in acidic Ca^{2+} stores and its association with plasma membrane Ca^{2+} channels upon acidic store depletion.

Blood was drawn from volunteers with local ethical committee approval. Cytosolic Ca^{2+} concentration ($[\text{Ca}^{2+}]_i$) measurement, immunoprecipitation and Western blotting were performed as previously described (Redondo *et al.*, 2006). Human platelets express STIM1 in lysosomes and lysosomal-related organelles, such as dense granules, isolated by immunomagnetic sorting. In dimethyl BAPTA-loaded cells, depletion of the acidic Ca^{2+} stores using the specific V-ATPase inhibitor, bafilomycin A1, or 2,5-di-(*t*-butyl)-1,4-hydroquinone (TBHQ), a SERCA3 inhibitor resulted in increased association between STIM1 and the capacitative Ca^{2+} -selective channel Orai1. Furthermore, treatment with TBHQ produced time-dependent co-immunoprecipitation of STIM1 or Orai1 with the TRPC proteins hTRPC1 and hTRPC6, which was found to occur independently of changes in $[\text{Ca}^{2+}]_i$. These results support the involvement of STIM1 in the activation of SOCE regulated by the acidic Ca^{2+} stores, and also the role of the channel proteins Orai1, hTRPC1 and hTRPC6 in Ca^{2+} entry after depletion of the acidic stores.

Rosado JA, Lopez JJ, Harper AG, Harper MT, Redondo PC, Pariente JA, Sage SO & Salido GM. (2004). *J Biol Chem* **279**, 29231-29235.

Redondo PC, Harper MT, Rosado JA & Sage SO. (2006). *Blood* **107**, 973-979.

Supported by MICINN grant BFU2010-21043-C02-01 and AECID-PCI A/023417/09. ND was supported by PRE09020.

Where applicable, the authors confirm that the experiments described here conform with The Physiological Society ethical requirements.

PC27

Preautonomic neurones of the paraventricular nucleus of the hypothalamus receive inputs from the cardiovascular region of the nucleus tractus solitarius

V.S. Affleck and S. Pyner

School Biological & Biomedical Sciences, University of Durham, Durham, UK

Control of the cardiovascular system is dependent upon a multisynaptic pathway that regulates sympathetic nerve activity. The paraventricular nucleus of the hypothalamus (PVN) and nucleus tractus solitarius (NTS) are critical components of the neural circuit that regulate sympathetic nerve activity³. The NTS projects to the PVN but there is no evidence to indicate this projection targets those preautonomic neurones in the PVN that regulate sympathetic activity. It is important to establish this as studies suggest elevated sympathetic nerve activity, strongly associated with cardiovascular disease including heart failure, is partly generated from the preautonomic neurones of the PVN³. The present study used anterograde (Biotin dextran amine-BDA) and retrograde (Fluorogold-FG or cholera toxin subunit B-CTB) labelling methods to identify the terminal neuronal targets of the ascending axonal projection from the NTS to the PVN.

All experiments were performed in accordance with the Animals (Scientific Procedures) Act, 1986. Studies were performed on male Wistar rats (n=8, 280-310 g). For anterograde labelling of NTS projecting axons, animals were anaesthetised using a combination of medetomidine (0.25 ml/100g) and ketamine (0.06 ml/100g). Animals received either an iontophoretic deposit or pressure injection (10 nl) into the NTS of 10 % BDA using the coordinates R/C -13.68 mm, L 0.5 mm and D/V -8.00 mm^{2,4,5}. After a recovery period (14 days) to allow anterograde transport of BDA to the PVN, animals were re-anaesthetised as previously described to allow an injection of either 1 µl of 2% FG or 5 µl of 0.5% CTB into the spinal cord to label spinally projecting preautonomic PVN neurones. Post-operatively during the recovery period, animal welfare was monitored with administration of analgesia (buprenorphine 0.1 ml/kg) as required. Following a 7-14 day recovery period animals were humanely killed (pentobarbital 60 mg/kg) perfused fixed (4% paraformaldehyde-PFA or 4% PFA and 0.5% glutaraldehyde) with removal of brain and spinal cord. Frozen sections (40 µm) were processed to reveal BDA and CTB^{1,4}. Tissues were examined under bright field or epifluorescence for the existence of putative connections between the NTS and the preautonomic neurones of the PVN.

The combination of techniques revealed ascending axons from the NTS that coursed through and around the PVN nucleus. The NTS terminals showed numerous varicosities, some of which appeared to closely appose the somata and dendrites of preautonomic spinally projecting PVN neurones.

This is the first demonstration that axonal fibres from the NTS target preautonomic neurones of the PVN. Functionally, this pathway has the potential to modulate the activity of those neurones controlling sympathetic outflow. It must also be considered that this pathway may contribute to the generation of abnormal sympathetic activity by the PVN.

Llewellyn-Smith IJ et al. (2005). *J Comp Neurol* 488, 278-289.

Paxinos G & Watson C (1998). *Stereotaxic atlas of rat brain*. Academic Press.

Pyner S (2009). *J Chem Neuroanat* 38, 197-208.

Pyner & Coote (1999). *Neuroscience* 88, 949-957.

Reiner A et al. (2000). *J Neurosci Methods* 1003, 23-37.

We gratefully acknowledge the British Heart Foundation for funding.

Where applicable, the authors confirm that the experiments described here conform with The Physiological Society ethical requirements.

Does the extracellular signal regulated kinase 1/2 (ERK1/2) contribute to the hormonal control of epithelial Na⁺ channel (ENaC) activity?

S. Simpson, M.K. Mansley and S.M. Wilson

Centre for Cardiovascular and Lung Biology, University of Dundee, Dundee, UK

ENaC-mediated absorption of Na⁺ in the distal nephron is crucial for whole body Na⁺ and water balance and therefore important to the control of blood pressure (Loffing and Korbacher, 2009). ENaC is regulated via complex mechanisms and studies of *Xenopus* oocytes expressing α -, β - and γ -ENaC indicate that phosphorylation of β - and γ -ENaC by ERK1/2 may restrict membrane Na conductance by facilitating the internalisation / degradation of ENaC subunits. ERK1/2 activity may thus contribute to the hormonal control of Na absorption (Yang et al., 2006), and the present study therefore explores the effects of an inhibitor of ERK1/2 (U0126) upon electrogenic Na⁺ transport in a mouse cortical collecting duct cell line (mpkCCD).

Cells grown to confluence on permeable membranes were therefore mounted in Ussing chambers where electrogenic Na⁺ transport was quantified using standard electrometric methods (see for example Manley & Wilson, 2010). Western analysis of extracted protein (n = 4) showed that U0126 (10 mM, 30 min) suppressed the phosphorylation of ERK1/2 at Tyr²⁰² / Tyr²⁰² indicating full inhibition of this kinase. Although U0126 (10 mM) also caused slight (5 – 10%) inhibition of amiloride-sensitive equivalent current (I_{Eq}), this effect was transient and, after 30 min, the electrical properties of control and U0126-treated cells were indistinguishable (Fig. 1). Basolateral insulin (20 nM, Fig 1A) and arginine vasopressin (AVP, 10 nM, Fig 1B) consistently augmented I_{Eq} and subsequent addition of apical amiloride (10 μ M) caused ~95% inhibition of the current recorded from hormone-treated cells indicating that these responses are due to increased Na⁺ absorption via ENaC. Western analysis (n = 4) showed that insulin (20 nM, 30 min) also stimulated the phosphorylation of an endogenous residue (PKB-Ser⁴⁷³) that is phosphorylated in a phosphoinositide-3-kinase (PI3K) -dependent manner but had no effect upon the phosphorylation of CREB-Ser¹³³, an endogenous protein kinase A (PKA) substrate. AVP, on the other hand, evoked phosphorylation of CREB-Ser¹³³ but not PKB-Ser⁴⁷³ (n = 4) and these hormones thus control ENaC activity via separate mechanisms involving PI3K and PKA respectively. Studies of U0126-treated cells revealed electrometric responses to insulin and AVP essentially identical to control (Fig. 1).

Despite the evidence implicating ERK1/2 in the control of ENaC activity (Yang et al., 2006), the present data show that complete inhibition of this kinase has no effect upon basal Na⁺ absorption and does not impair PI3K or PKA-dependent control of ENaC in mpkCCD cells.

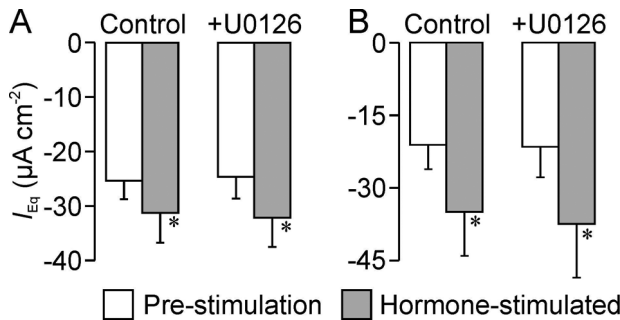


Figure 1. Confluent mpkCCD cells were mounted in Ussing chambers, allowed to stabilise for approximately 40 min and then exposed to 10 μM U0126 (+U0126) or solvent vehicle (control) for 30 min. The cells were then stimulated with either insulin (A, 20 nM, basolateral, n = 5) or arginine vasopressin (B, 10 nM, basolateral, n = 5). Open columns show equivalent currents (I_{Eq}) monitored under open circuit conditions that were quantified immediately before the cells were exposed to hormones, whilst shaded columns show currents recorded after 30 min stimulation. Data are mean \pm s.e.m. and asterisks denote statistically significant ($P < 0.05$, Student's paired t test) effects of hormones upon I_{Eq} .

Loffing J & Korbacher C. (2009) *Pflügers Arch* **458**, 111-135.

Mansley MK & Wilson SM. (2010) *Br J Pharmacol* **161**, 571-588.

Yang L-M, Rinke R & Korbacher C. (2006) *J Biol Chem* **281**, 9859-9868.

Supported my an MRC doctoral training award (MKM).

Where applicable, the authors confirm that the experiments described here conform with The Physiological Society ethical requirements.

PC29

Phosphorylation of STIM1 in tyrosine residues is required during the activation of SOCE in human platelets

E. López, A. Berna-Erro, G.M. Salido, J.A. Rosado and P.C. Redondo

Physiology, University of Extremadura, Cáceres, Extremadura, Spain

Stromal interaction molecule 1 (STIM 1) has been described to communicate the content of the stores to plasma membrane channels during store operated calcium entry (SOCE) in a number of cells, including human platelets (Ong et al. 2007). STIM1 EF-hand domain detects intraluminal calcium levels and allows STIM multimerization into puncta in close apposition to calcium channels in the plasma membrane, such as canonical TRP or Orai proteins. (Ong et al. 2007; Muik et al 2009) STIM 1 can be regulated by Ser and Pro phosphorylation (Manji et al. 2000; Smyth et al. 2008). Hence we have investigated whether STIM1 could also be regulated by phosphorylation in Tyr residues during SOCE activation.

Blood samples from healthy donors were obtained according to the Declaration of Helsinki and platelets were isolated as previously described (Rosado and Sage 2000). Fura 2-loaded platelets were stimulated with thapsigargin (TG, 200 nM) and calcium mobilization was registered using the rapid kinetics Stop flow system. Subsequently, platelets were stimulated with TG (200 nM) by using a Quench flow system and fixed by mixing with RIPA at different stimulation times. STIM1 was immunoprecipitated from platelet lysates using 2 µg/mL anti-GOK/STIM1 antibody (overnight at 4°C). SDS-PAGE and Western blotting using a specific anti-phosphotyrosine antibody (4G10) revealed that maximal STIM1 tyrosine phosphorylation was detected 2.5 s after addition of TG. STIM1 maximal phosphorylation time-point was not modified upon removal of extracellular or both extra- and intracellular calcium with either EGTA (100 µM) alone or in combination with dimethyl BAPTA (loading with dimethyl BAPTA-AM 10 µM for 30 min).

Finally, platelets suspended in absence or presence of calcium, were treated with the dual Src/Lyn inhibitor, Bosutinib (1,5 µM) for 30 min at 37 °C, resulting in the inhibition of STIM1 tyrosine phosphorylation, an effect that was found to be greater in the presence of calcium, which indicate that Src family members, such as pp60^{src}, might be involved in STIM1 tyrosine phosphorylation during the activation of SOCE. TG-evoked SOCE resulted significantly reduced in presence of bosutinib, thus suggesting that STIM1 tyrosine phosphorylation plays a functional role in SOCE in human platelets.

Ong et al., (2007). J. Biol. Chem.; 282:12176-85.

Smyth JT et al., (2008). Nat. Cell. Biol 11, 1465-72.

Manji SS et al., (2000). Biochim. Biophys. Acta 1481, 147-55.

Muik M et al., (2009). J. Biol. Chem 284, 8421-6.

Rosado JA & Sage SO (2000). J Biol Chem 276, 15659-65.

This work is supported by MEC (BFU2010-21043-C02-01), AECID-PCI (A/023417/09) and UEX (novel investigation program A-VII). Redondo PC is supported by RYC program (RYC-20070-00349), Lopez E is supported by Carlos III health program (FI10/00573) and Berna-Erro A is supported by UEX (D-01).

Where applicable, the authors confirm that the experiments described here conform with The Physiological Society ethical requirements.

PC30

Lack of effect in vivo of K⁺-channel modulators on jejunal fluid absorption after *Escherichia coli* toxin (STa) challenge

M.L. Lucas, L.C. Gilligan, C. Whitelaw, P.J. Wynne and J.D. Morrison

University of Glasgow, Glasgow, UK

A prevalent model for diarrhoeal disease (1) envisages enterocyte chloride ion secretion into the lumen, on the assumption that enterocytes work in reverse and secrete

as well as absorb. Heat stable STa toxin from E.coli is thought to conform to this model but in vivo loops fail to secrete on exposure to toxin, although inhibited absorption is found (5). A sub-hypothesis of the electrogenic secretion model is that secretion is assisted by enterocyte membrane potential being maintained by K⁺ channel opening to allow luminal chloride ion exit. The hypothesis that K⁺ channel blockers, glibenclamide and clotrimazole should restore fluid absorption and cromakalim should worsen fluid absorption inhibited by STa was tested in vivo in rat jejunum. Fluid uptake was measured (2) in anaesthetised (70 mg/kg i.p Sagatal) unfasted Sprague-Dawley female rats using recovered volume. Twenty five loops were perfused with 100 mM NaHCO₃/54 mM NaCl, with 80 ng/ml E. coli STa, with or without 300 uM glibenclamide, 50 uM clotrimazole or 2 uM cromakalim intraluminally or 30 mg/Kg i.v. glibenclamide, 50 mg/Kg i.v. clotrimazole or 5 ug/Kg i.v. cromakalim. After experiment, animals were humanely killed. Results are given as the mean fluid absorption (ul/cm/hr) with standard error of the mean, plus number of animals. One loop was used per experiment. Significance was by 't' test, correcting for multiple comparisons.

Net fluid absorption was 98.8 ± 8.8 (9) ul/cm/hr in control perfused jejunal loops and was 38.5 ± 4.2 (8) ul/cm/hr in loops perfused with STa. Co-perfusion with 300 uM glibenclamide or with 50 uM clotrimazole, concentrations identified (3) as inhibiting STa mediated elevations in short-circuit current and proposed as anti-secretory compounds, had no effect on STa inhibited fluid absorption when measured in vivo. The K⁺ channel opener also did not alter inhibited fluid absorption although identified as anti-secretory (4). Intravenous perfusion was also without effect on fluid absorption inhibited by STa, although anticipated vasomotor effects namely hypotension in the cases of clotrimazole and cromakalim and a mild pressor effect with glibenclamide were found. Our findings are that K⁺ channel regulators are unable to affect fluid absorption that has been inhibited by E.coli STa. These experiments challenge a further aspect of the dogma of enterocyte chloride ion secretion being the basis for the diarrhoeal disease when the intestine is exposed to STa.

Field, M. (2003) Intestinal ion transport and the pathophysiology of diarrhea. J Clin Invest 111: 931-943.

Fedorak, R. N. & Allen, S. L. (1989). Effect of somatostatin analog (SMS 201-995) on in vivo intestinal fluid transport in rats. A limited systemic effect. Digestive diseases and sciences. 34: 567-572.

Devor, D. C. et al. (1997). Inhibition of intestinal Cl⁻ secretion by clotrimazole: direct effect on basolateral membrane K⁺ channels. Am J Physiol 273: C531-C540.

Schirgi-Degen, A. & Beubler, E. (1996). Involvement of K⁺ channel modulation in the proabsorptive effect of nitric oxide in the rat jejunum in vivo. Eur J Pharmacol 316: 257-262.

Lucas, M. L. (2010) Enterocyte secretion: a doctrine untroubled by proof Exp Physiol 95: 471-485.

Where applicable, the authors confirm that the experiments described here conform with The Physiological Society ethical requirements.

Mechanical Properties of Bilipid Layers for a Bioinspired Mechanoreceptor

X. Duan¹, S. Arnold¹, M.C. Rosamond¹, J. Atherton¹, A.J. Gallant¹, S. Pyner² and S. Johnstone¹

¹*School of Engineering and Computing Sciences, Durham University, Durham, UK and*

²*Biological and Biomedical Sciences, Durham University, Durham, UK*

This study aims to understand the structure and mechanical characteristics of bilipid membranes for an artificial mechanoreceptor. This includes defining Young's modulus and bending rigidity. Three types of lipid molecule, L- α -phosphatidylcholine (Egg-PC), 1,2-dioctadecanoyl-sn-glycero-3-phosphocholine (DSPC) and 1,2-didodecanoyl-sn-glycero-phosphocholine (DLPC) (Avanti Polar Lipids, Inc.,) are being used for comparison in both vesicle and bilipid planar forms. These were chosen since they have different lipid tail lengths such that gel and fluid phases can be compared (Goertz et al., 2009). The bilipid membranes have been fabricated on supporting mica substrates such that their dynamic and static stress responses can be studied using Atomic Force Microscopy.

Nanometre unilamellar vesicles were prepared by dissolving lipid powder in chloroform, evaporating the organic solvent using a dry nitrogen stream and then drying in a desiccator connected to a rotary vacuum pump. The resulting lipid film was hydrated and sonicated to produce vesicles with a range of diameters. These were re-suspended by stirring them in an aqueous buffer solution (0.5 mg/ml) and sonicated to clarity. The resulting vesicles were then deposited onto a mica surface within a water filled fluid cell of an Atomic Force Microscope (Veeco Multimode E®) (AFM) at room temperature. The concentration and fluid cell flow rate determines the resulting formation. i.e. vesicle or planar bilayer.

A scanned image of a planar bilayer of Egg-PC on a mica substrate in deionised water is shown in Figure 1a. The section analysis displays a membrane thickness of 3.8 nm \pm 0.6nm, confirming the presence of a bilayer. This is consistent with the literature where values range from 3.9nm \pm 0.4nm to 5nm \pm 1nm (Liang et al 2004, Reviakine et al., 2000). A similar technique was applied using DSPC and DLPC. High yield fabrication of reliable bilayer structures is needed for sensor development with yields presently as low as 33% (Pioufle et al., 2008).

To measure the bending rigidity of vesicle structures, the AFM is used to produce force-distance curves. A Hertz contact model assuming a spherical shape for both the tip and vesicle (Liang et al., 2004) is then applied. A softer rounded AFM tip has been fabricated by locally depositing platinum on top of standard silicon nitride cantilevers in a Focussed Ion Beam (FIB) system (Figure 1b). This enables a Hertz model to be applied to planar membranes (Lebedev et al., 2009) to measure Young's modulus.

To conclude, methods to measure the mechanical and structural properties of bilipid structures have been developed. However, fabrication yield needs to be improved to produce repeatable structures to develop a viable sensing mechanism.

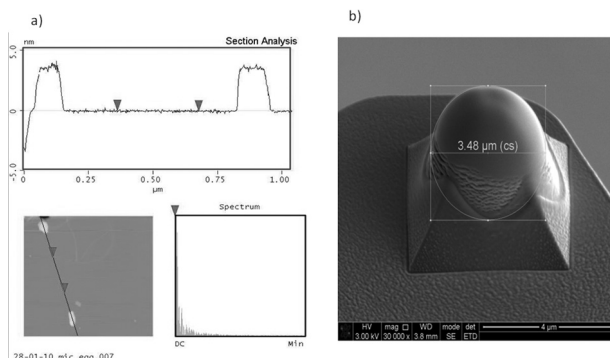


Figure 1: a) Section view, plan view and spatial spectrum of Egg-PC planar layer partially coating mica substrate b) Platinum Coated Silicon Nitride AFM tip for planar membrane testing

Lebedev DV, Chuklanov AP, Bukharaev AA et al, Technical Physics Letters, 35(4), 371-374, 2009.

Liang X, Mao G, Ng KYS, Colloids and Surfaces B: Biointerfaces 34, 41-51, 2004.

Le Pioufle B, Suzuki H., Tabata KV et al, Anal. Chem, 80, 328-332, 2008.

We gratefully acknowledge EPSRC for funding and advice from Dr Kataky.

Where applicable, the authors confirm that the experiments described here conform with The Physiological Society ethical requirements.

PC32

NMDA receptor subunit expression in the paraventricular nucleus of the spontaneously hypertensive (SHR) and pregnant rat

S.C. Cork, P.L. Chazot and S. Pyner

School of Biological and Biomedical Sciences, University of Durham, Durham, UK

Hypertension and pregnancy are accompanied by an increase in sympathetic nerve activity (SNA) to regions of the cardiovascular system. The paraventricular nucleus of the hypothalamus (PVN) has previously been shown to be a critical centre for control of the sympathetic nervous system and there is evidence to suggest the PVN plays a role in the sympathoexcitation noted in these states¹.

Evidence indicates there is an increased glutamatergic influence within the PVN of heart failure (HF) and hypertensive animals^{1,2}. Within the PVN of rats in HF, there is an increased expression of the NR1 subunit of the NMDA receptor that is correlated with sympathoexcitation¹. Studies in pregnant animals are yet to confirm whether NMDA plays a role in sympathoexcitation.

We hypothesise the sympathoexcitation observed in hypertension and pregnancy is a result of an alteration in NMDA receptor subunit expression that may confer a functional consequence.

All experiments were performed in accordance with the Animals (Scientific Procedures) Act, 1986. A total of 12 animals were used in these studies (4 female Wistar (200g), 4 pregnant Wistar (E19) and 4 female SHR (14 weeks)). Animals were humanely killed with sodium pentobarbital (60mg/kg). The brains were removed and frozen in iso-pentane and stored at -80°C. The PVN was located³ and bilateral punches were taken. Tissue was dissolved in sample buffer and frozen at -20°C. Quantitative immunoblotting was performed using SDS-PAGE (10% acrylamide gel). Immunoblots were probed with 1 µg/ml of either rabbit anti-NR1 or rabbit anti-NR2A (2 days, 4°C) followed by incubation with anti-rabbit IgG and then normalised against β -actin⁴. Results were quantified based on their optical densitometry using imageJ. We have confirmed the presence of the NR1, NR2A, NR2B and NR2C/D subunits within the PVN of normotensive, hypertensive and pregnant rats. For the SHR and pregnant animals, there was no change in expression levels for the NR1 and NR2A receptor subunit compared with the normotensive controls. This is the first demonstration that expression levels of the NR1 and NR2A subunits are not altered in the SHR or pregnant animal. This data suggests these NMDA receptor subunits may not contribute to the increased SNA observed in pregnancy and hypertension. In relation to NR1 subunit expression, this data differs from that reported in the PVN of heart failure animals¹. However it is the NR2 subunits which confer receptor functionality. Further investigation is required to determine the significance of these findings with respect to receptor function and sympathetic over activity.

Li *et al.*, (2003) *Circ Res*: 93; 990-997.

Li *et al.*, (2008) *J Physiol*: 586(6); 1637-1647.

Paxinos & Watson (1998) *Academic Press*.

Thompson *et al.*, (2002) *Brain Res Mol Brain Res*. 102(1-2):55-61.

This work was supported by the BBSRC.

Where applicable, the authors confirm that the experiments described here conform with The Physiological Society ethical requirements.

PC33

Tamoxifen: chondroprotective effects post-mechanical trauma

E.L. Parker, C. Peetroons, S.J. Getting, F. Hucklebridge and M.J. Kerrigan

School of Life Sciences, University of Westminster, London, UK

Mechanical trauma through repetitive, high-impact sport contributes to the onset of osteoarthritis. Mechanical trauma disrupts cell cytoskeletal organization (Blain, 2009), which is important in maintaining cell integrity. Since tamoxifen has been shown to have anti-calmodulin effects (Hall *et al.* 1999), acting upstream of actin regulatory proteins, this study was designed to investigate whether this compound exerts a chondro-protective effect following mechanical trauma.

Cartilage explants were dissected from the joints of 18-21 month old steers (obtained from a local abattoir) into DMEM. Explants were incubated for 1h in either: isotonic (280mOsm), hypertonic (380 mOsm) or tamoxifen (10 μ M) supplemented DMEM and subsequently subjected to a single impact as previously described (Bush et al., 2005). Chondrocyte viability, volume and relative F-actin concentration were determined by confocal microscopy and data expressed as mean \pm s.e.m; (Student's t-test: $p < 0.05$), $n = 45$ cells each from 3 distinct experiments.

Explants in isotonic DMEM exhibited a decrease in cell viability from $85 \pm 0.05\%$ to $45 \pm 2.52\%$ at 48h post impact; $p < 0.05$. Conversely, when incubated with hypertonic DMEM or 10 μ M tamoxifen there was no significant decrease in chondrocyte viability from $90 \pm 3.65\%$ and $95 \pm 4.51\%$ to $90 \pm 2.63\%$ and $88 \pm 3.34\%$ respectively at 48h. Tamoxifen incubated samples displayed a decrease in cell volume ($p < 0.01$) from $716 \pm 23 \mu\text{m}^3$ to $424 \pm 16 \mu\text{m}^3$ at time 0, when compared to control conditions. However explants incubated in isotonic and hypertonic DMEM all exhibited an impact-induced decrease in cell volume 48hrs post impact, from $716 \pm 23 \mu\text{m}^3$ and $578 \pm 31 \mu\text{m}^3$ to $516 \pm 15 \mu\text{m}^3$ and $302 \pm 12 \mu\text{m}^3$ ($p < 0.05$) respectively, whereas tamoxifen incubated explants displayed no significant decrease in cell volume post-impact, from $424 \pm 16 \mu\text{m}^3$ to $432 \pm 5 \mu\text{m}^3$. Additionally pre-incubation with tamoxifen resulted in an decrease ($p < 0.05$) in F-actin:volume ($0.75 \pm 0.04\text{AU}$) when relative to non-treated samples prior to mechanical trauma, conversely hypertonic pre-incubation displayed an increase ($p < 0.05$) in F-actin:volume ($1.21 \pm 0.06\text{AU}$). Interestingly, explants pre-treated with isotonic and hypertonic DMEM all exhibited an impact-induced decrease ($p < 0.01$) in F-actin:volume to $0.58 \pm 0.03\text{AU}$ and $0.73 \pm 0.04\text{AU}$ respectively at 48hrs post impact, relative to non-treated samples prior to mechanical trauma. Conversely tamoxifen treated explants showed no significant change in F-actin:volume at 48hrs ($0.73 \pm 0.04\text{AU}$).

These data suggest that tamoxifen exhibits a chondro-protective effect in an in vitro model of mechanical trauma by inhibiting impact-induced cell volume and F-actin decrease.

Blain, E.J., Int. J. Exp. Path, 2009. 90: p. 1–15.

Bush P et al. (2005). Osteoarthritis Cartilage 13, 54-65.

Hall, AC., et al., 45th Annual Meeting, Orthopaedic Research Society, Anaheim, California.

I would like to acknowledge the University of Westminster for funding my PhD, my supervisory team for their guidance, the other members of the ORL; Miss Y Nedelcheva, Dr A Qusous and Miss M Kaneva as well and the honour students for their collaborative minds.

Where applicable, the authors confirm that the experiments described here conform with The Physiological Society ethical requirements.

Exploring the Effects of Non-Thermal Infrared Irradiation on an Alzheimer's Disease Mouse Model

N.A. Duggett, S.L. Burroughs and P.L. Chazot

School of Biological & Biomedical Sciences, Durham University, Durham, UK

Non-thermal infrared (IR) wavelengths (700-1100nm) have been shown to elicit a broad range of physiological effects and therapeutic benefits, including modulation of many cellular processes involved in the progression of ageing¹. It has been widely postulated that a primary photoacceptor for IR lies within the mitochondria and stimulation initiates retrograde signalling, enabling mitochondria-nucleus communication, influencing a plethora of cellular processes^{2,5}. Our research focuses on 1072nm, a wavelength at the peak of IR transmission through water and thus high tissue penetrability¹. Previously we have reported chronic exposure *in vivo* significantly improved learning performance in a premature ageing, CD-1 mouse model³. Recent unpublished studies from our laboratory have shown IR1072 treatment reduced A β 42 expression and plaques in TASTPM Alzheimer's disease model mice, in a gender-dependent manner.

All experiments were performed in accordance with the Animals (Scientific Procedures) Act, 1986.

TASTPM (GSK, UK), were exposed to sham or IR1072nm treatment for 6 minutes for 2 successive days, biweekly over 5 months, equipment temperature was continually monitored. Parallel sham treatments were undertaken in replica apparatus which did not emit IR1072nm. (n=3-4 per group)

Mice were humanely killed, decapitated, brain tissue dissected, homogenised and subjected to quantitative immunoblotting probing with rabbit anti-HSP27 (Heat Shock Protein-27), HSP70 or HSP105 (1:125, 2 days, 4°C) antibodies, normalised against mouse anti- β -actin (1:3000, overnight, 4°C). Results were quantified using ImageJ to measure optical densitometry.

Mitochondria from the brain and liver of non-treated mice were isolated and Complex I and II activity of the respiratory chain measured using the polarographic method⁴. Data were analysed using a non-parametric Student's two tailed T-test. (n=3-6 replicates)

We have found significant effects in TASTPM mice, with an apparent down-regulation of HSP105 (p<0.001) and HSP70 (p<0.001) in IR treated males and upregulation of HSP70 (p<0.05) in IR treated females but no respective change in HSP105 expression.

Preliminary results showed that female TASTPM mice had higher respiratory complex activity and a higher RCI (respiratory control index) than their male counterparts. This may explain sexual dimorphism in HSP70 and A β 42 expression; increased mitochondrial activity can lead to AP-1 (activator protein-1) induction, which induces transcription factors resulting in DNA synthesis and thus increased protein levels^{2,5}.

Further investigation is required to determine whether such high complex activity is maintained or even increased further in IR treated female TASTPM mice to determine the role of the mitochondria in HSP activation.

Bradford, A., Barlow, A. & Chazot, P. L. (2005) *Journal of Photochemistry and Photobiology B: Biology*, **81**, pp 9-14

Karu, T. I. (2008) *Photochemistry and Photobiology* **84**, pp 1091-1099

Michalikova, S., Ennaceur, A., van Resberg, R. & Chazot, P. L. (2008) *Neurobiology of Learning and Memory*, **89**, pp 480-488

Chance, B. and Williams, G. R. (1956) *Advances in Enzymology and Related Subjects of Biochemistry*, **17**, pp 65-134.

Gao, X., Xing, D. (2009) *Journal of Biomedical Science*, 16(4)

This project has been supported by Bionet/CELS (SB), Virulite, BSI and a Durham Seedcorn Postgraduate grant (ND)

Where applicable, the authors confirm that the experiments described here conform with The Physiological Society ethical requirements.

PC35

Mechanical loading activates Indian Hedgehog signalling and modulates primary cilia length

C. Davis^{1,2}, P. Chapple² and M. Knight¹

¹*School of Engineering and Materials Science, Queen Mary University of London, London, UK* and ²*Centre for Endocrinology, William Harvey Research Institute, Queen Mary University of London, London, UK*

Hedgehog signalling is aberrantly activated in osteoarthritis (OA) a chronic degenerative disease that affects articular cartilage [1]. Hedgehog signalling requires the primary cilium [2]. The majority of chondrocytes possess a cilium and cilia incidence and length is increased in osteoarthritic cartilage compared with healthy cartilage [3]. In this study we investigated the hypothesis that Indian Hedgehog (Ihh) gene expression is regulated by mechanical loading in mature articular chondrocytes and that changes in primary cilia length and prevalence influence the capacity of these cells to respond to Hh signals.

Articular chondrocytes were harvested from bovine metacarpal-phalangeal joints obtained from an abattoir. Chondrocytes were subjected to cyclic tensile strain using the Flexcell 4000T system and stimulated with 5, 10 or 20% strain at 0.33Hz for 1hr. Primary cilia incidence and length were quantified using confocal images of cells labelled with acetylated α -tubulin ($n > 300$ cells). Quantitative real-time PCR was used to monitor Ihh gene expression and the expression of Patched1 (Ptch1) which provides a measure of Hh pathway activation. For these experiments $n = 5$ replicates with cells pooled from 3 different animals. Statistical analysis was conducted using t-tests.

Mechanical loading induced a dose dependant reduction in primary cilia length compared to unloaded controls with statistically significant differences following loading at 10% and 20% strain. Loading had no effect on cilia prevalence. *Ihh* gene expression was up-regulated only at 10% strain ($p<0.05$). This was associated with an increase in *Ptch1* gene expression ($p<0.05$) which also occurred at 5% strain ($p<0.05$). We have shown for the first time that *Ihh* exhibits magnitude dependent mechanosensitive expression in mature articular chondrocytes and that mechanical loading induces changes in chondrocyte primary cilia length. Hh pathway activation was observed at 5% strain, despite no significant changes in *Ihh* expression. This suggests that mechanical loading may also be inducing the release of endogenous *Ihh*. The lack of pathway activation at 20% may be due to reduced cilia length as well as a lack of *Ihh* expression. Understanding Hh regulation in mature chondrocytes is essential for development of future pharmaceutical treatments for OA based on manipulation of Hh signalling.

Lin AC et al. (2009). Modulating hedgehog signaling can attenuate the severity of osteoarthritis. *Nat Med* 15, 1421-5.

Corbit KC et al. (2005). Vertebrate Smoothed functions at the primary cilium. *Nature* 437, 1018-21.

McGlashan SR et al. (2008). Primary cilia in osteoarthritic chondrocytes: from chondrons to clusters. *Dev Dyn* 237, 2013-20.

C.Davis is funded by a BBSRC studentship.

Where applicable, the authors confirm that the experiments described here conform with The Physiological Society ethical requirements.

PC36

GH improves endothelial function & lipid profile but increases RPP & PIIP in drug users

M.R. Graham¹, P.J. Evans², B. Davies³, F.M. Grace⁴ and J.S. Baker⁴

¹Health & Exercise Science, Glyndwr, Wrexham, UK, ²Diabetes & Endocrinology, Royal Gwent Hospital, Newport, UK, ³Health & Exercise Science, Glamorgan University, Pontypridd, UK and ⁴Sport & Exercise Science, University of the West of Scotland, Hamilton, UK

Background: In hypertensive subjects without a history of overt cardiovascular disease (CVD), arterial pulse wave velocity (APWV) is a surrogate measure of arterial stiffness, arterial endothelial dysfunction and CVD and independently predicts the occurrence of cardiovascular events (Boutouyrie, et al, 2002).

Amino-terminal propeptide of type III procollagen (PIIP) is increased in plasma and arterial aneurysm tissue compared with healthy arterial tissue (Ihara et al., 2004). Anabolic-androgenic steroid (AAS) drug use combined with strength training independently predisposes to endothelial dysfunction and decreased arterial compliance (Kasikcioglu et al., 2007).

Objectives: To establish if recombinant human growth hormone (rhGH) in an AAS group affected endothelial function, rate pressure product, lipid profile and PIIP, compared with a control group.

Methods: Male subjects (n=48) were randomly divided, using a single blind procedure into two groups: (1): control group (C) n=24, mean \pm SD, age 32 ± 11 years; height 1.8 ± 0.06 metres; 2): rhGH using group ($0.019 \text{ mg.kg}^{-1}.\text{day}^{-1}$) (GH) n=24, mean \pm SD, age 32 ± 9 years; height 1.8 ± 0.07 metres. Physiological responses, anthropometry, arterial pulse wave velocity (APWV), blood pressure (BP), heart rate (HR), and biochemical indices were investigated.

Results: Body mass index, fat-free mass index significantly increased, body fat significantly decreased within GH (all $P < 0.017$). Insulin like growth factor-I and PIIP significantly increased within GH ($P < 0.017$) and compared with C ($P < 0.05$). Serum sodium significantly increased ($P < 0.017$) and serum homocysteine, and high sensitivity C-reactive protein, significantly decreased within GH (all $P < 0.017$).

Arterial pulse wave velocity, significantly decreased within GH ($P < 0.017$) and compared with C ($P < 0.05$). Total cholesterol, triglycerides and low density lipoprotein all significantly decreased within GH ($P < 0.017$). Resting HR and rate pressure product (RPP) significantly increased within GH ($P < 0.017$) and compared with C ($P < 0.05$).

Conclusion: The elevation in PIIP supports previous research in the area (Velloso et al., 2006). RhGH therapy has been shown to improve cardiovascular risk factors in strength training athletes, using AAS (Graham et al, 2007), however the current study suggest that short term use of rhGH although having beneficial effects on endothelial function, lipoprotein profile and specific inflammatory markers of cardiovascular disease in AAS drug users, may controversially also have an adverse effect on the cardiovascular system, as evidenced by the increase in resting RPP and PIIP and should therefore not be recommended in drug users.

Control group vs. Growth Hormone Administration group (GH)

Variables	Control Group			Administration Group		
				(PRE-GH)	(on-GH)	(POST-GH)
Day	1	7	14	1	7	14
Body Fat	21.9 ± 3.8	21.7 ± 3.8	21.6 ± 4.0	20.0 ± 6.0	19.0 ± 6.0*	19.1 ± 5.8*
FFMI	21.8 ± 2.1	21.8 ± 2.1	21.8 ± 2.1	21.9 ± 1.9	22.3 ± 1.9*	22.0 ± 1.9¥
LL PRE-OCC VELOCITY	9.81 ± 1.62	9.83 ± 1.50	9.85 ± 1.54	9.97 ± 1.38	9.18 ± 1.6*†	9.26 ± 1.52*
HR	66 ± 16	67 ± 16	67 ± 14	70 ± 6	78 ± 5*†	71 ± 6
SBP	125 ± 12	124 ± 12	125 ± 11	126 ± 10	125 ± 12	122 ± 9
RPP	83 ± 22	84 ± 24	85 ± 22	88.2 ± 9	97.5 ± 8*†	86.6 ± 9
Sodium (mmol/L)	139.6 ± 8.4	141.5 ± 3.1	140.5 ± 5.8	140.6 ± 2.7	142 ± 2.4*	140 ± 2.4
TC (mmol/L)	4.4 ± 1.0	4.6 ± 0.9	4.5 ± 1.1	4.7 ± 0.9	4.4 ± 0.7*	4.7 ± 1.0
TG (mmol/L)	1.0 ± 0.4	1.1 ± 0.5	1.1 ± 0.4	1.4 ± 0.4	1.1 ± 0.3*	1.4 ± 0.4
HDL (mmol/L)	1.2 ± 0.4	1.3 ± 0.3	1.2 ± 0.3	1.2 ± 0.3	1.2 ± 0.2	1.2 ± 0.3
LDL (mmol/L)	2.7 ± 0.8	2.8 ± 0.8	2.8 ± 1.0	2.9 ± 0.3	2.5 ± 0.3*	2.9 ± 0.3
hsCRP(mg/L)	1.35 ± 1.9	1.38 ± 2.1	1.44 ± 2.1	1.77 ± 2.1	1.29 ± 1.6*	1.7 ± 2.8
HCY (µmol/L)	12.5 ± 4.2	13.3 ± 4.7	13.1 ± 4.1	13.2 ± 4.0	11.7 ± 3.1*	13.1 ± 4.3
IGF-I (ng/ml)	179 ± 47	169 ± 50	175 ± 53	159 ± 54	323 ± 93*†	175 ± 61¥
PIIIP (U/ml)	0.32 ± 0.1	0.30 ± 0.1	0.32 ± 0.1	0.28 ± 0.1	0.42 ± 0.2*†¥	0.35 ± 0.1*

Figures are presented as means ± Standard Deviations (SD)

Body fat (%); FFMI = Fat free mass index (kg.m⁻²); LL PRE-OCC VELOCITY, Lower Limb Pre-occlusion Velocity (m.s⁻¹); Heart rate (HR; bpm), Systolic Blood Pressure (SBP; mm.Hg), and Rate Pressure Product (RPP; bpm.mmHgX10⁻²); TC = Total Cholesterol; TG = Triglycerides; HDL = High Density Lipoprotein; LDL = Low Density Lipoprotein; hsCRP = highly selective C-reactive Protein; HCY = Homocysteine; IGF-I = Insulin like growth Factor-I;

PIIIP = Amino-terminal propeptide of type III procollagen

* = P<0.017, significantly different to PRE-GH;

¥ = P<0.017, significantly different to on-GH;

† = P<0.05 significantly different to C group.

Table. Control group vs. Growth Hormone Administration group (GH).

Variables	Control Group			Administration Group		
	(PRE-GH)	(on-GH)	(POST-GH)			
Day	1	7	14	1	7	14
Body Fat	21.9 ± 3.8	21.7 ± 3.8	21.6 ± 4.0	20.0 ± 6.0	19.0 ± 6.0*	19.1 ± 5.8*
FFMI	21.8 ± 2.1	21.8 ± 2.1	21.8 ± 2.1	21.9 ± 1.9	22.3 ± 1.9*	22.0 ± 1.9*
LL PRE-OCC VELOCITY	9.81 ± 1.62	9.83 ± 1.50	9.85 ± 1.54	9.97 ± 1.38	9.18 ± 1.6*†	9.26 ± 1.52*
HR	66 ± 16	67 ± 16	67 ± 14	70 ± 6	78 ± 5*†	71 ± 6
SBP	125 ± 12	124 ± 12	125 ± 11	126 ± 10	125 ± 12	122 ± 9
RPP	83 ± 22	84 ± 24	85 ± 22	88.2 ± 9	97.5 ± 8*†	86.6 ± 9
Sodium (mmol/L)	139.6 ± 8.4	141.5 ± 3.1	140.5 ± 5.8	140.6 ± 2.7	142 ± 2.4*	140 ± 2.4
TC (mmol/L)	4.4 ± 1.0	4.6 ± 0.9	4.5 ± 1.1	4.7 ± 0.9	4.4 ± 0.7*	4.7 ± 1.0
TG (mmol/L)	1.0 ± 0.4	1.1 ± 0.5	1.1 ± 0.4	1.4 ± 0.4	1.1 ± 0.3*	1.4 ± 0.4
HDL (mmol/L)	1.2 ± 0.4	1.3 ± 0.3	1.2 ± 0.3	1.2 ± 0.3	1.2 ± 0.2	1.2 ± 0.3
LDL (mmol/L)	2.7 ± 0.8	2.8 ± 0.8	2.8 ± 1.0	2.9 ± 0.3	2.5 ± 0.3*	2.9 ± 0.3
hsCRP (mg/L)	1.35 ± 1.9	1.38 ± 2.1	1.44 ± 2.1	1.77 ± 2.1	1.29 ± 1.6*	1.7 ± 2.8
HCY (μmol/L)	12.5 ± 4.2	13.3 ± 4.7	13.1 ± 4.1	13.2 ± 4.0	11.7 ± 3.1*	13.1 ± 4.3
IGF-I (ng/ml)	179 ± 47	169 ± 50	175 ± 53	159 ± 54	323 ± 493*†	175 ± 61*
PIIIP (U/ml)	0.32 ± 0.1	0.30 ± 0.1	0.32 ± 0.1	0.28 ± 0.1	0.42 ± 0.2*†	0.35 ± 0.1*

Figures are presented as means ± Standard Deviations (SD)

Body fat (%); FFMI = Fat free mass index ($\text{kg}\cdot\text{m}^{-2}$); LL PRE-OCC VELOCITY, Lower Limb Pre-occlusion Velocity ($\text{m}\cdot\text{s}^{-1}$); Heart rate (HR): bpm, Systolic Blood Pressure (SBP: mm.Hg), and Rate Pressure Product (RPP: $\text{bpm}\cdot\text{mmHg}\times 10^{-3}$); TC = Total Cholesterol; TG = Triglycerides; HDL = High Density Lipoprotein; LDL = Low Density Lipoprotein; hsCRP = highly selective C-reactive Protein; HCY = Homocysteine; IGF-I = Insulin like growth Factor-I; PIIIP = Amino-terminal propeptide of type III procollagen

* = $P < 0.017$, significantly different to PRE-GH;

† = $P < 0.017$, significantly different to on-GH;

‡ = $P < 0.05$ significantly different to C group.

Boutouyrie P et al, (2002). Hypertension 39, 10–15.

Ihara A et al, (2004). Pathophysiol Haemost Thromb 33, 221–224.

Kasikcioglu E et al, (2007). Int J Cardiol 114, 132–134.

Graham MR et al, (2007). Growth Horm IGF Res 17, 201–209.

Velloso et al, (2006). Communication to the Physiological Society, C48.

Drug Control Centre, King's College London

Where applicable, the authors confirm that the experiments described here conform with The Physiological Society ethical requirements.

PC37

Mechanical Stress impairs Keratinocyte Migration

A. Vollmers, N. Fullard, T. Hoehner and J. Reichelt

Dermatological Sciences, Newcastle University, Newcastle upon Tyne, UK

Keratinocytes sense mechanical loading (1). While activation upon mechanical stress has only been studied in primary keratinocytes, the response of keratinocyte stem

cells remains unknown. Our hypothesis is that keratinocyte stem cells are more resistant to strain than their progeny in order to maintain their quiescent state. In this study, we aimed to establish how stretch influences murine keratinocyte stem cells migration.

Murine keratinocytes isolated from neonatal mice can be grown as keratinocyte lines with indefinite replicative potential (2). Like primary keratinocytes these lines express keratin 5, whereas keratin 6 expression is strongly decreased. The stem cell marker keratin 15 which is restricted to few cells in primary cultures is highly expressed in keratinocyte lines (85%). Keratinocyte lines retain the capacity to differentiate and stratify in high calcium medium.

We found that, similar to human keratinocytes (3), mouse keratinocytes grow clonally in culture, giving rise to holo- (HC), mero- (MC) and paraclones (PC), of which HC consist of keratinocyte stem cells. This allowed us to isolate keratinocyte stem cells by their phenotype.

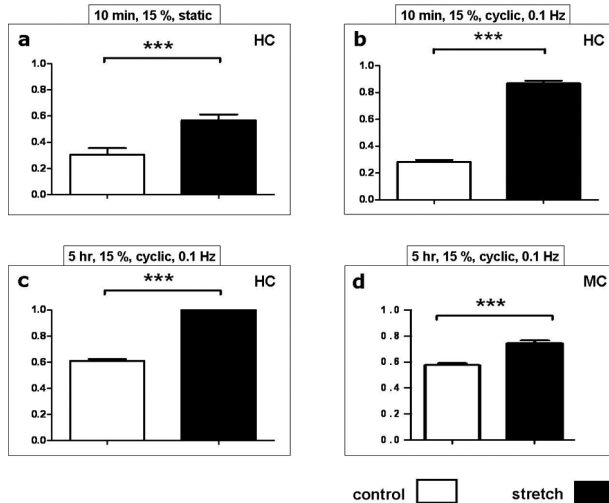
Keratinocyte monolayers enriched in HC, were grown on six-well plates with a flexible silicone bottom. Monolayers were scratched with a yellow pipette tip. Using a computer controlled stretch system (Flexcell) uniaxial 15% stretch was applied: 10 min static or cyclic stretch at 0.1 Hz and wound closure was assessed after 8 hours. Keratinocyte stem cells (HC) migrated slower upon stretch than unstretched controls. This effect was more pronounced under cyclic (50%) compared to static stretch (23%).

Continuous cyclic stretch for 5 hours completely inhibited keratinocyte stem cell (HC) migration, whereas cultures consisting of more differentiated keratinocytes (MC) were able to migrate into the wound gaps although they migrated 15% slower than unstretched control cells.

Cultures were treated with mitomycin C for 2 h before the start of the experiments. One way ANOVA was used for statistical analysis, $p < 0.001$, $n = 10$.

Our data show that established murine keratinocyte lines represent a valuable source for keratinocyte stem cells. Using the Flexcell system we demonstrated that mechanical stress impairs keratinocyte migration. This effect was more pronounced under permanent cyclic stretch than under static stretch. Furthermore undifferentiated keratinocyte stem cells (HC) were more affected by mechanical stress than cultures containing a higher proportion of differentiated keratinocytes (MC).

The results indicate that mechanical load inhibits keratinocyte migration and that keratinocyte stem cells are affected more than differentiated keratinocytes.



Reichelt J (2007). *Europ J Cell Biol* **86**, 807-816.

Reichelt J & Haase I (2009). *Methods in Molecular Biology* **585**, 59-69.

Barrandon Y & Green H (1987). *Proc Natl Acad Sci USA* **84**, 2302-2306.

This research was funded by the German Research Foundation.

Where applicable, the authors confirm that the experiments described here conform with The Physiological Society ethical requirements.

PC38

CB1/CB2 cannabinoid receptors regulate basal salivation and protein-electrolyte saliva content in submandibular salivary gland

O. Netsyk¹, O. Kopach² and N. Fedirko¹

¹Ivan Franko National University of L'viv, L'viv, Ukraine and ²Bogomoletz Institute of Physiology NASU, Kiev, Ukraine

Cannabinoid receptors (CBRs) belong to G protein-coupled receptor superfamily. CBRs expression was suggested for the submandibular cells however their role in the acinar cell physiology remains unclear.

Experiments were performed on male Wistar rats. The rats were anesthetized with i.p. injection of pentobarbital (30–40 mg/kg). Saliva was collected using variable speed peristaltic pump. The effectiveness of basal salivation was evaluated by saliva flow rate, concentration of total proteins, α -amylase activity and concentration of electrolytes (Ca^{2+} , Na^+ , K^+ , P) in saliva collected from the ducts in oral cavity before and after administration of cannabinoids. Submandibular cells were isolated by col-

lagenase digestion. *In vitro* we measured Na^+/K^+ -ATPase activity in the submandibular acinar cell's microsomal fraction.

We showed that activation *in vivo* of CB1R and CB2R of submandibular salivary gland with selective agonist WIN 55212-2 (5 μM) caused suppression of basal salivation and alteration of saliva content. Similar changes were observed after single administration of cannabinoid and in the conditions of prolonged drug use. Maximal inhibition of basal salivation we observed in 10 min after single application of WIN 55212-2 (~ 45%) and ~ 60% – in the conditions of prolonged administration of an agonist. Prolonged treatment with WIN 55212-2 leads to acidification of secreted saliva (by 0,5-0,8 pH u). Any significant changes of K^+ , Na^+ , P concentrations in final saliva were observed upon activation of CBRs. Repetitive application of WIN 55212-2 also induced an increase of both calcium and proteins concentrations in saliva. An increase of total protein concentration began at 10 min ($52 \pm 9\%$ of saline-treated group; $n = 10$, $p < 0.05$) and was increased for all period tested ($72 \pm 9\%$ of saline-treated group at 15 min; $n = 9$, $p < 0.05$); α -amylase activity was increased by $25 \pm 5\%$, $p < 0.05$, $n = 12$. A significant increase of calcium concentration began at 20 min ($47 \pm 5\%$ of saline-treated group; $n = 8$, $p < 0.05$) and lasted for 30 min during a repetitive WIN 55,212-2 application. We also showed that decrease of basal salivation is accompanied by inhibition of Na^+/K^+ -ATPase activity (by $41 \pm 6\%$, $p < 0.05$, $n = 7$).

Therefore upon activation of CBRs: i) the activity of cAMP-mediated signaling system that contribute to the protein secretion is increased; ii) transcellular H_2O transport that contribute to the fluid secretion is reduced forming the base of inhibition of basal salivation; iii) electrolyte saliva content remains unaltered suggesting an unaltered functioning of the ductal cells unlike acinar cells. Concluding, observed changes of saliva pH and Na^+/K^+ -ATPase activity in acinar cells contribute to the CBRs-mediated inhibition of basal salivation by submandibular gland.

Where applicable, the authors confirm that the experiments described here conform with The Physiological Society ethical requirements.

PC39

Whirlin function in proprioceptive mechanotransduction

J.C. de Nooij¹, A. Simon³, S. Doobar^{1,2}, K.P. Steel⁴, R.W. Banks⁵, G.S. Bewick³ and T.M. Jessell^{1,2}

¹Dept. of Biochemistry and Molecular Biophysics, Columbia University, New York, NY, USA, ²Howard Hughes Medical Institute, New York, NY, USA, ³School of Medical Sciences, University of Aberdeen, Aberdeen, UK, ⁴Wellcome Trust Sanger Institute, Wellcome Trust Genome Campus, Cambridge, UK and ⁵School of Biological & Biomedical Sciences, University of Durham, Durham, UK

Proprioceptive sensory feedback is critical for many aspects of motor control. This form of sensory feedback derives largely from specialized mechanoreceptors located within muscles: the muscle spindle (MS; responsive to changes in muscle length)

and the Golgi tendon organ (GTO; responsive to changes in muscle tension) (1). Anatomical and physiological analysis has provided insight into the sensory transduction process in MS and GTO afferents and has demonstrated that the afferent stretch response is primarily carried by sodium currents (2). The stretch-evoked MS-afferent impulse frequency is significantly diminished by amiloride, implicating the Degenerin/ENaC family of sodium channels as components of the MS-afferent mechanotransduction channel (3). Glutamate, released from sensory terminals, tonically maintains afferent excitability, possibly by regulating membrane insertion of mechano-transduction channels (4). Despite these recent advances, the molecular mechanisms that underlie the transformation of proprioceptive mechanical stimuli into electrical impulses remain largely unknown.

In a molecular screen for new proprioceptor specific molecules, we recently found that whirlin is selectively expressed in proprioceptive sensory neurons in dorsal root ganglia. Whirlin encodes a scaffold protein with important roles in hair cell and photoreceptor sensory transduction (5), raising the possibility that whirlin also functions in the proprioceptive mechanotransduction process. Using an in vitro muscle/nerve preparation, we find that the activation of spindle afferents by mechanical stretch is compromised in whirlin mutant mice when compared to heterozygous mice. Application of exogenous glutamate normalizes afferent stretch-sensitivity. These observations suggest that essential components of the proprioceptive transduction machinery are inefficiently 'deployed' in whirler mutant mice. Given that whirlin contains three PDZ-domains, and is known to recruit macromolecular complexes to specific subcellular locations, we speculate that whirlin may function to recruit and/or ensure the proper subcellular localization of a mechano-transduction complex in proprioceptive sensory terminals. Our current studies are aimed at testing this hypothesis.

The identification of whirlin provides opportunities to identify additional components of the proprioceptive transduction machinery. The parallel expression of whirlin in proprioceptive muscle afferents, hair cells and photoreceptor cells raises the possibility of a central role for whirlin in diverse sensory transduction processes.

Windhorst, U. (2007). *Brain Res Bull*, 73: 155-202.

Hunt, CC. (1990). *Physiol Rev*. 70: 643-63.

Simon et al. (2010). *J Physiol*. 588: 171-85.

Bewick et al. (2005). *J Physiol*. 562: 381-94.

Mburu et al. (2003). *Nat Genet*. 34: 421-8.

Where applicable, the authors confirm that the experiments described here conform with The Physiological Society ethical requirements.

PC40

REV5901: an investigation on the chondroprotective effect in bovine chondrocytes following single impact trauma

Y. Nedelcheva, S.J. Getting and M.J. Kerrigan

School of Life Sciences, University of Westminster, London, UK

Chondrocytes, the sole resident cell-type in cartilage are responsible for the maintenance of the extracellular matrix and as they do not divide it is vital to find a protective mechanism against impact trauma. A single impact load to a joint causes subchondral bone fracture resulting in permanent cartilage damage to the ECM, including surface fissures, loss of proteoglycan, cell death and pre-disposition to osteoarthritis (Bush *et al.*, 2005, Scott & Athanasiou, 2006).

Full-depth cartilage was excised from bovine metacarpal-phalangeal joints (18-24 months of age, obtained from a local abattoir) under aseptic conditions. Explants were incubated with 5 μ M calcein-AM and 1 μ M propidium iodide and impact experiments were performed by drop-tower with a single impact of 0.131J. Samples were incubated alone or in the presence of REV5901 (50 μ M), Wortmannin (10nM) and Uridine (100 μ M). Cell viability was determined time points of 0, 5, 10, 20 & 30 mins post impact by confocal laser scanning microscopy (CLSM). Data for cell volume was determined in non-impacted samples and 30 min post impact. Western blot analysis were used to determine alterations in actin binding proteins. Protein bands were analysed by Image J software and changes in expression quantified. All data are expressed as Mean \pm s.e.m. *P<0.05 vs. control, n = 4 determination in triplicate.

Impact led to cell death which was significantly reduced by a pre-incubation with REV5901 from 10.92 \pm 1.02% to 5.44 \pm 0.59% (p<0.001). Samples treated with Uridine caused a reduction of cell death that was significantly lower from the control samples 8.10 \pm 0.40% (p<0.05) but couldn't reach the chondro-protective effect offered by REV5901 (p<0.01). In contrast, samples treated with Wortmannin increased cell death to 12.02 \pm 1.83%. Cell death was significantly reduced in samples treated in combination of Wortmannin and REV5901 8.58 \pm 0.54%. Data for volume changes showed significant decrease in volume for cell treated with Wortmannin 359.9 \pm 17.67 μ m³, compared to 716.136 \pm 37.81 μ m³ and 552.68 \pm 27.26 μ m³ for control (p<0.001) and REV5901 (p<0.001). Nevertheless, cell volume for cells treated with Uridine significantly decreased in comparison to the control 608.3 \pm 24.32 μ m³ (p<0.05). In addition, when cells were treated with a combination of Wortmannin and REV5901 cell volume size was restored to 538.09 \pm 30.6 μ m³. Western blot analysis showed that only cofilin and gelsolin from the actin binding proteins were expressed in all the samples, no profilin or phospho-cofilin were detected.

These data confirm the therapeutic opportunities offered by REV5901 and it's chondro-protective properties in part due to the polymerisation of the actin cytoskeleton. We suggest that the pathway involved via the phosphoinositide 3-kinases (PI3Ks)

could offer novel therapeutic opportunities for prevention of irreversible cartilage damage from acute impact trauma.

Bush, P, *et al.*, (2005). Viability and volume of *in situ* bovine articular chondrocytes—changes following a single impact and effects of medium osmolarity. *Osteoarthritis and Cartilage*. **13**(1), 54-65

Scott, C, Athanasiou, K (2006). Mechanical impact and articular cartilage. *Critical reviews in bio-medical engineering*. **34**(5), 347-378.

Where applicable, the authors confirm that the experiments described here conform with The Physiological Society ethical requirements.

PC41

***Melissa officinalis* L. Essential Oil contains a novel Voltage-gated sodium channel blocker with anticonvulsant potential**

G. Lees^{3,2}, R. Abuhamdah¹, I. Hoskin³, L. Huang³, C. Dixon³, C. Breen³, S.Y. Han³, W. Connolly³, M. Carroll⁵, M.J. Howes⁴, M. Mahita⁶ and P. Chazot¹

¹Biological & Biomedical Sciences, Durham University, Durham, UK, ²School for Health, Durham University, Durham, UK, ³Department of Pharmacology and Toxicology, University of Otago, Dunedin, New Zealand, ⁴Jodrell Laboratory, Royal Botanic Gardens, Kew Gardens, Kew, UK, ⁵Chemistry Department, University of Newcastle, Newcastle-upon-Tyne, UK and ⁶Sunderland Pharmacy School, University of Sunderland, Sunderland, UK

Melissa oil is the essential oil extracted from the leaves of *Melissa officinalis* L. (Lamiaceae). Melissa is used in traditional aromatherapy to alleviate depression, anxiety, stress and insomnia. We have identified Melissa oil as an effective depressant of neurotransmission, with a proposed mechanism involving voltage-gated sodium channels (VGSCs)(1).

Melissa essential oil (Mo) reversibly blocks 750 ms bursts of sustained repetitive firing in cultured forebrain cells from E16-18 Sprague-Dawley rats without any effect on the primary spike. Voltage-clamp experiments in N1E 115 neuroblastoma cells confirmed that Mo (0.1-1 mg/ml) was able to block VGSCs and exert hyperpolarising shifts in the fast inactivation curves which were significantly greater than those evoked by supra-clinical concentrations of carbamazepine (100 µM). High frequency stimulation and depolarisation both facilitated the blocking action of Mo, and Mo reversibly reverses ictal-like epileptiform activity in a 4-AP (4-aminopyridine)-induced brain slice model for epilepsy(2). Based on a [³H] batrachotoxinin A 20- α -benzoate binding assay (3), Mo was confirmed to modulate VGSCs, but the 12 most common components within the oil appeared not to modulate VGSCs.

Essential oils are characterized by a very complex mixtures whose components belong to different classes of compounds including hydrocarbons, aldehydes, ketones, esters, and alcohols that range widely in concentration and variability among different plant species. A solid phase extraction protocol (SPE) was developed as an initial step for identifying the neuroactive components in Mo. 100 µL of the essential

oils was loaded onto a 4g silica cartridge (SF10-4g) that had previously been conditioned with pentane. The elution of the SPE cartridge was performed using a vacuum manifold at a velocity of 3 ml/sec with the following solvent sequence: Fraction I: pentane 100% Fraction II: pentane/ethyl ether 90:10 and Fraction III: ethyl ether 100%. Gas chromatography mass spectroscopy (GC-MS) analysis was carried out on Melissa essential oil and the three fractions. Fraction A contained all hydrocarbons; fraction B carbonyl compounds, ethers, esters and tertiary alcohols; Fraction C primary alcohols, acids and diols. This method was successful in fractionating Essential oils into three distinct fractions in one simple step easily, quickly and using small amounts of organic solvents. Protocols have been modified to further improve the fractionation profiles, and the fractions are now being tested using our electrophysiological and binding assays.

Abuhamdah S *et al* (2008) *J Pharm Pharmacol* **60** 377-84.

Lees G *et al* (2005) *Neuropharmacology* **50** 98-110

Duan Y *et al* (2005) *Eur J Pharmacol* **530** 9-14

This work was funded in part by the Alzheimer's Society (UK) and Durham University Wolfson Institute

Where applicable, the authors confirm that the experiments described here conform with The Physiological Society ethical requirements.

Function and regulation of ENaC and ASICs

S. Kellenberger

Université de Lausanne, Lausanne, Switzerland

The epithelial Na⁺ channel / degenerin superfamily of ion channels comprises Na⁺ channels involved in various cell functions in Metazoa. Its members include the degenerins involved in touch sensitivity in *C. elegans*, Pickpocket and related channels in *D. melanogaster*, the peptide-gated FANaC ion channels of the nervous system of mollusks, as well as the Epithelial Na⁺ channel (ENaC) and proton-activated acid-sensing ion channels (ASICs) which are both found in mammals. ENaC mediates Na⁺ transport in epithelia and is essential for sodium homeostasis (1). ASICs are present in the central and peripheral nervous system where they have different physiological and pathological functions, as the expression of fear, the sensation of pain and neurodegeneration after ischemia (2). All ENaC/degenerin family members are Na⁺-selective or -preferring ion channels with relatively low unitary conductance, and many have been shown to be inhibited by the diuretic amiloride. Biochemical and functional studies indicated that ENaC/degenerin channels are multimeric proteins whose subunits have two transmembrane domains, short intracellular N- and C-termini and a large extracellular part. The recently published crystal structure of ASIC1 showed a trimeric channel of the proposed subunit organization. Degenerins have been shown to form the channel part of a mechanotransduction complex in *C. elegans*, touch neurons. In analogy, a possible mechanosensitivity of ASICs and ENaC has been investigated. To date there is much evidence supporting an involvement of ASICs in mechanosensation, however the exact role of ASICs in mechanosensation is unclear. ENaC is a constitutively active channel, whose contribution to Na⁺ transport is regulated on the level of the expression of the protein, as well as by many modulators of channel activity, as for example proteases and Na⁺ ions. For ASICs, the only identified direct activators so far are protons. The ASICs are therefore considered as ligand-gated channels. We have recently applied a systematic approach to identify potential pH-sensing residues in ASIC1a. We calculated the pK_a of all extracellular His, Glu and Asp residues using a Poisson-Boltzmann continuum approach based on the ASIC 3D structure, to identify candidate pH-sensing residues. The role of these residues was then assessed by site-directed mutagenesis and functional analysis (3). The localization of putative pH-sensing residues suggests that pH changes control ASIC gating by protonation / deprotonation of many residues per subunit in different channel domains, thus that protons act differently from larger ligands which bind to a low number of distinct binding sites. In conclusion, members of ENaC/degenerin subfamilies share a similar structural organization; however they differ in their activators and physiological roles. It is likely that parts of the gating machinery are common between different subfamily members.

Schild, L. (2010) Biochim Biophys Acta 10.1016/j.bbadis.2010.06.014

Wemmie, J. A., Price, M. P., and Welsh, M. J. (2006) Trends Neurosci 29, 578-586

Liechti, L. A., Berneche, S., Bargeton, B., et al. (2010) J Biol Chem 285, 16315-16329

Where applicable, the authors confirm that the experiments described here conform with The Physiological Society ethical requirements.

SA02

TRP channels as sensors and transducers in the vasculature

D. Beech

University of Leeds, Leeds, UK

One of the outstanding challenges of biological science is to understand the nature, regulation and physiological importance of the various non-selective, calcium- and sodium-permeable cationic channels contained within blood vessels. One reason why this is important is because of the hypothesis that the channels are central to mechanical- and lipid- sensing or transduction; fundamental, enigmatic and interconnected aspects of vascular biology. Candidates for the molecular basis of the underlying channels are the Transient Receptor Potential proteins (TRPs), which are encoded by 28 genes in mammals and generate extensive additional diversity through heteromultimeric assembly. The heteromultimers, still poorly defined in physiology, redundancies within assemblies and intricate and, again poorly defined, relationships with other proteins in restricted sub-cellular spaces (often dominated by cytoskeleton) are challenges that have emerged and prevented straightforward understanding. In this situation, simple molecular deletion, knock-down and over-expression of single TRPs may often be inadequate as experimental strategies. There are also difficulties in defining the appropriate physical and lipid manipulations to mimic the relevant physiological contexts, which include luminal pressure, disturbed shear stress, physical injury, and directional sensing requirements of cell migration and proliferation as blood vessels form and remodel. Despite such complexities, there are tantalising indications that various TRPs are involved (1-5). That almost all TRP subtypes have been implicated may be a reflection of physiological realities, such as needs for back-up systems and multiple sensors and transducers with varied mechanical and lipid sensitivities. The lecture will review data on TRPs in this biological context and outline emerging hypotheses for how the proteins may contribute.

Muraki et al (2003). Circ Res. 93, 829-38.

Inoue et al (2009). Circ Res. 104, 1399-409.

AbouAlaiwi et al (2009). Circ Res. 104, 860-9.

Ma et al (2010). Arterioscler Thromb Vasc Biol. 30, 851-8.

Al-Shawaf et al (2010). Arterioscler Thromb Vasc Biol. 30, 1453-9.

Our research is funded by the Wellcome Trust, British Heart Foundation and Medical Research Council.

Where applicable, the authors confirm that the experiments described here conform with The Physiological Society ethical requirements.

SA03

The mechano-gated K_{2p} channels: focus on TREK-1

E. Honoré

Institut de Pharmacologie Moléculaire et Cellulaire, Valbonne, France

Two-pore-domain K⁺ (K2P) channel subunits are made up of four transmembrane segments and two pore-forming domains that are arranged in tandem and function as either homo- or heterodimeric channels. This structural motif is associated with unusual gating properties including background channel activity and sensitivity to membrane stretch. Moreover, K2P channels are modulated by a variety of cellular lipids and pharmacological agents, including polyunsaturated fatty acids and volatile general anesthetics. Recent *in vivo* studies have demonstrated that TREK-1, the most thoroughly studied K2P channel, has a key role in the cellular mechanisms of neuroprotection, anaesthesia, pain and depression.

Where applicable, the authors confirm that the experiments described here conform with The Physiological Society ethical requirements.

SA04

Caveolae and signal transduction in muscle

T. Burkholder

Georgia Institute of Technology, Georgia, GA, USA

Caveolae are flask-shaped invaginations of the cell membrane present in most mechanically active cells. These structures may behave like two-dimensional springs and represent mechanotransduction organelles. Although a lipid bilayer is nearly inextensible, the cell membrane is capable of large changes in area during cell stretch or membrane tether extension. Bending of caveolae may provide the required change in apparent surface area. This suggests that caveolae concentrate mechanical deformations, serving as mechanical amplifiers while simultaneously reducing tension in the rest of the plasma membrane. The morphology of caveolae is dependent on a coating of caveolin protein on the inner surface, and deformation of the caveolae changes the interaction between caveolin monomers. Caveolin is a scaffolding molecule and organize src, ERK, and NOS signaling cassettes, and may link activation of those cassettes to mechanotransduction. The caveolin-1 (cav1) dependent caveolae of endothelial cells have been linked to transduction of shear and swelling stresses via NOS and chloride channels, although the stretch response seems to be independent of cav1. The assembly of signaling cassettes may be necessary for proper

transmission of biochemical signals, independent of any deformation. Mature skeletal muscle expresses primarily caveolin-3 (cav3), which associates with dystrophin at membrane overlaying the Z-disc. The cav3 dependent caveolae link src kinase with multiple effectors, including TRPC1 channels and confer redox sensitivity to the channel, independent of mechanical stimulation. To determine whether caveolin-dependent signaling results derive from mechanical properties of caveolae or from the scaffolding function of caveolins is quite difficult, because interventions that disrupt caveolin-mediated scaffolding also disrupt the morphology of caveolae. However, the structural arrangement of caveolae is highly suggestive of direct mechanical effects that may be revealed by careful mechanical testing. For example, skeletal myoblasts have a viscoelastic response response to cyclic stretch that is consistent with simultaneous caveolae-resident and -nonresident mechanical sensors. This suggests that controlling the dynamic conditions of mechanical stimulation may emphasize effects related to deformation of caveolae over effects related to caveolin scaffolding.

Where applicable, the authors confirm that the experiments described here conform with The Physiological Society ethical requirements.

SA05

β ENaC in VSMC function: importance in renal myogenic constriction, renal injury, and hypertension

H. Drummond, S. Grifoni and D. Stec

University of Mississippi Medical Center, Jackson, MS, USA

Renal blood flow (RBF) autoregulation is mediated by two overlapping mechanisms, the fast acting myogenic response and the slower tubuloglomerular feedback (TGF). The fast acting myogenic response is thought to prevent transmission of systemic pressure to the renal microvasculature and prevent renal injury and related hypertension. Despite the physiological importance of the myogenic response, the molecular identity of the elements transducing vascular stretch into a cellular event remains unclear. Several candidates have been considered as transducers of vascular stretch into intracellular signaling. Our laboratory has focused on Epithelial Na⁺ Channel (ENaC) proteins because of their strong evolutionary link to mechanotransduction in the nematode, *C. elegans*. Previous studies from our lab suggest β protein (β ENaC) plays an important role in myogenic constriction in certain arteries. Silencing of endogenous β ENaC (siRNA, genetically modified mice) inhibits myogenic constriction. Mice with reduced levels of β ENaC (β ENaC m/m) have delayed whole kidney autoregulatory responses, even in the presence of active TGF, suggesting defective myogenic autoregulation. When TGF is suppressed following blood volume expansion, renal autoregulation is inhibited. In the absence of TGF, autoregulatory index at 2 min was significantly higher in the β ENaC m/m mice ($+0.45 \pm 0.26$ vs. -0.66 ± 0.32 , $p=0.0099$). β ENaC m/m mice have increased expression of inflammatory and

remodeling markers, such as macrophage infiltration, IL1- β , IL6, TNF α collagen III and TGF β . Furthermore, β ENaC m/m mice increased mean arterial blood pressure (MAP, 120 ± 3 vs. 105 ± 2 mm Hg, $p=0.016$), as measured using radio telemetry. Our findings suggest β ENaC is an important mediator of renal myogenic constriction mediated RBF autoregulation *in-vivo* and loss of the myogenic mechanism is associated with early signs of renal injury and increased MAP.

Where applicable, the authors confirm that the experiments described here conform with The Physiological Society ethical requirements.

SA07

Mechanotransduction in bone and the role of glutamate signalling

T. Skerry

Mellanby Bone Centre, University of Sheffield, Sheffield, UK

While it is clear that the skeleton is responsive to the demands imposed on it by habitual activity, the complexity of the response of bone to loading is not immediately apparent. Since the goal of adaptive changes in bone is the production of a structure that will resist loads with some adequate margin for safety, there will be different solutions in different bones. It is therefore important to consider what sort of loading is experienced by a bone physiologically, as the mass and architecture will depend on the combination of loading experience superimposed upon some genetically determined minimal baseline structure. We know for example that bones respond to high magnitudes of load more than low, high rates of strain change more than slow rates, and it is possible that bone is more sensitive to high frequencies of loading than low. Interestingly though after a relatively small number of load cycles, the response of bone to a given loading regimen becomes saturated so that larger numbers of cycles in the same bout do not increase the response. If however a saturating number of cycles is divided into several bouts in a single day, then that division causes a potentiated response which is greater than the same number in a single bout. This potentiation means that some evidence of earlier bouts of loading is retained by the skeleton which influences the effect of later bouts. The mechanism behind such a "memory" for exercise in bone is unknown. Some years ago, in an attempt to understand adaptive signalling mechanisms better, we used a subtractive technique (differential RNA display) and showed regulated expression of a component of a glutamatergic synapse in osteocytes a few hours after loading *in vivo*. This led us to explore expression of a range of molecules associated with glutamate signalling in the CNS, in bone cells, and we have shown that all cells in bone express such molecules to a greater or lesser degree. *In vitro* studies have shown that glutamate signalling is involved in both bone formation and resorption, but *in vivo* studies have been problematic, because of difficulties with drugs that cross the blood-brain barrier and affect behaviour. However recent studies using tissue specific gene knockouts have begun to yield data. One essential component of a glutamatergic synapse in the CNS is the NMDA type receptor – a glutamate gated channel. The

NMDA receptor is a heteromer, comprising NMDA receptor 1 subunits and one of 4 NMDA receptor 2 subunits. The NMDA receptor 1 subunit (now known as Grin1 for glutamate receptor ionotropic – NMDA) is considered obligate and its deletion ablates NMDA receptor signalling in the CNS. By crossing a floxed Grin1 mouse with either osteocalcin or tartrate resistant acid phosphatase Cre strains, we have deleted Grin1 in osteoblasts and osteoclasts respectively. Surprisingly the phenotype of the OCCre-Grin1 flox mice is variable and mild, despite clear evidence for a role for glutamate in osteoblast differentiation *in vitro*. However, mice lacking Grin1 in osteoclasts and their precursors have evidence of tibial flare, and osteosclerosis, suggesting that absence of glutamate receptors in those cells affects their function significantly. Our current working hypothesis is that glutamate release by osteocytes and osteoblasts regulates bone resorption and contributes to the mechanism by which bone tunes its structure to activity.

Where applicable, the authors confirm that the experiments described here conform with The Physiological Society ethical requirements.

SA08

PKG and osteoblast mechanotransduction

R. Pilz

University of California, San Diego, La Jolla, UK

Mechanical stimulation of bone cells is critical for maintaining bone mass and strength, and a better understanding of how mechanical stimuli are converted into intracellular signals to activate an anabolic program in osteoblasts/cytes is fundamental to improving treatments for osteo-degenerative diseases (1;2). Weight bearing and locomotion stimulate interstitial fluid flow through the bone canalicular system, and the resultant shear stress is thought to be a major mechanism whereby mechanical forces stimulate osteoblast/osteocyte growth and differentiation (1;2). In primary osteoblasts and osteoblast/cyte-like cell lines, we found that fluid shear stress induced rapid expression of c-fos, fra-1, fra-2, and fosB/ Δ fosB mRNAs (3); these genes encode transcriptional regulators important for osteoblast proliferation and differentiation, as demonstrated by the phenotypes of mice that over-express or lack these proteins, respectively (4). Fluid shear stress increased osteo-blast nitric oxide (NO) synthesis, leading to increased cGMP synthesis and activation of cGMP-dependent protein kinases (PKGs). Pharmacological inhibition of the NO/cGMP/PKG signaling pathway blocked shear-induced expression of all four fos family genes. Induction of these genes required signaling through MEK/Erk, and Erk activation was NO/cGMP/PKG-dependent. Treating cells with a membrane-permeable cGMP analog partly mimicked the effects of fluid shear stress on Erk activity and fos family gene expression, and cGMP's effects were enhanced by increased intracellular calcium, as occurs in mechanically-stimulated osteoblasts. In cells transfected with siRNAs specific for membrane-bound PKG II, shear- and cGMP-induced Erk

activation and fos family gene expression was nearly abolished and could be restored by transducing cells with a virus encoding an siRNA-resistant form of PKG II; in contrast, siRNA-mediated repression of the more abundant cytosolic PKG I isoform was without effect. We further demonstrated that PKG II mediates the fluid shear-induced increase in osteoblast proliferation. We have identified a mechanism whereby PKG II activates Erk and induces proliferation in osteoblasts, which includes PKG II regulation of c-Src and cross-talk between NO/cGMP/PKG and integrin signaling. PKG II-null mice show defective osteoblast Src/Erk signaling, and decreased Erk-dependent gene expression in bone; previous studies in NO synthase-deficient mice have demonstrated an important role of NO in osteoblast biology (5). We now establish a central role of NO/cGMP/PKG II signaling in osteoblast mechano-transduction, and propose a model whereby NO/cGMP/PKG II-mediated Src and Erk activation and induction of fos family genes play a key role in the osteoblast anabolic response to mechanical stimulation.

Ehrlich, P. J. and Lanyon, L. E. (2002) Osteoporosis. *Int.* 13, 688-700

Ozcivici, E., Luu, Y. K., Adler, B., Qin, Y. X., Rubin, J., Judex, S., and Rubin, C. T. (2010) *Nat. Rev. Rheumatol.* 6, 50-59

Rangaswami, H., Marathe, N., Zhuang, S., Chen, Y., Yeh, J. C., Frangos, J. A., Boss, G. R., and Pilz, R. B. (2009) *J. Biol. Chem.* 284, 14796-14808

Wagner, E. F. and Eferl, R. (2005) *Immunol. Rev.* 208, 126-140

Armour, K. E., Armour, K. J., Gallagher, M. E., Godecke, A., Helfrich, M. H., Reid, D. M., and Ralston, S. H. (2001) *Endocrinology* 142, 760-766

Where applicable, the authors confirm that the experiments described here conform with The Physiological Society ethical requirements.

SA09

The role of the cytoskeleton in osteocyte mechanotransduction

A. Bakker

ACTA - VU University Amsterdam, Amsterdam, Netherlands

Healthy bones combine a proper resistance against fracture with a minimum use of material. This property is brought about by osteocytes in response to mechanical cues, but it is still unknown how whole bone loads are translated into a signal that can be sensed by the osteocytes. Osteocytes form an network of stellate cells embedded within the calcified bone matrix (1). It is assumed that osteocytes are unable to directly sense the tiny loading-induced deformations of this matrix, but it has been shown that matrix deformations can drive a flow of interstitial fluid over the osteocytes, which could amplify the mechanical signal. Endothelial cells are activated when the fluid flow produces a shear stress on the cell membrane. It seemed logical to assume that shear stress is responsible for activation of mechanically stimulated osteocytes as well. Theoretical models predicted that daily mechanical loads would provoke shear stresses on the osteocytes that were sufficient in magnitude

to be sensed (2), but lately the accuracy of these calculations are under debate. As an alternative “amplification mechanism” it was proposed that fluid flow-induced drag forces on fibers that tether the osteocyte process to the matrix may be more important than fluid shear stress for activating the osteocyte, but the existence of these fibers has not been proven. It has also been suggested that the osteocyte processes are attached to the apex of infrequent, previously unrecognized conical projections in the matrix via integrins. A theoretical model predicts that these integrins provide stable attachment for the range of physiological loadings (3). However, we applied ultra high voltage electron microscope tomography to reconstruct 3-D images of osteocyte cell processes and did not observe “conical projections”, nor did we observe direct contact between the osteocyte process and the bone matrix. So it is still a mystery which molecular features are responsible for transducing loading-derived fluid flows into a signal that activates the osteocytes. That is, if current dogma that fluid flow activates osteocytes in response to bone loading is correct. Matrix deformations of 0.1% induce a fluid flow in bones, but deformations of this magnitude occur very rarely in mammalian bones. In addition, we recently found that osteocytes in mice with a genetic deletion that renders the osteocytes almost devoid of cell fingers may still be mechanosensitive. This reopens the discussion whether fluid flow is the manner of bone mechanotransduction, because physics laws dictate that loading-induced fluid flows will only occur around the osteocyte cell fingers. Osteocytes express a single primary cilium that projects from the surface of the cell body (4), and the cilium could act as a vibration sensor or a sensor of hydrostatic pressure providing an alternative for the fluid flow hypothesis. Given the crucial importance of osteocytes for maintaining a proper resistance against bone fracture, it seems obvious that a much greater knowledge of the molecular mechanisms that govern the adaptive response of osteocytes in their natural 3D surroundings is needed.

Klein-Nulend J and Bakker AD. *Clinic Rev Bone Miner Metab* 5 Edited by Dan Bikle, pages 195-209, 2007

Weinbaum S, Cowin SC, Zeng Y. *J Biomech* 27, 339–360, 1994

Wang Y, McNamara LM, Schaffler MB, Weinbaum S. *Proc Natl Acad Sci USA* 104, 15941-15846, 2007

Malone AMD, Anderson CT, Tummala P, et al. *Proc Natl Acad Sci USA* 104, 13325-13330, 2008

Where applicable, the authors confirm that the experiments described here conform with The Physiological Society ethical requirements.

SA10

Deconstructing Pain and Touch Sensation with *Caenorhabditis elegans*

M.B. Goodman

Molecular and Cellular Physiology, Stanford University, Stanford, CA, CA, USA

The ability to detect touch is conserved from echinoderms to humans. It relies on specialized mechanoreceptor neurons that vary in their sensitivity and association with accessory structures. Despite its importance and conservation across taxa, very little is known about how touch works. We seek to improve understanding by studying the nematode *C. elegans*, a simple animal that has only 30 mechanoreceptor neurons. Our work focuses on two classes of mechanoreceptor neurons: the 6 non-ciliated touch receptor neurons (TRNs) that detect touch applied to the body wall (1, 2) and the paired ciliated ASH neurons that detect noxious mechanical stimuli applied to the nose. Genetic analysis has revealed ion channel genes needed for TRN and ASH function. To learn the precise cellular function of such channel proteins and to investigate their gating mechanisms, we combine genetic dissection with *in situ* electrophysiology and biomechanical analysis. The picture emerging from our recent work is that touch activates similar ion channels in the nonciliated TRNs and the ciliated ASH neurons, which differ by 100-fold in their sensitivity to external force. Challenges for the future include understanding the basis for differences in sensitivity and the biophysics of mechanotransduction channel gating.

O'Hagan R, Chalfie M, Goodman MB (2005) *Nat Neurosci* 8:43-50Cueva JG, Mullholland A, Goodman MB (2007) *J Neurosci* 27: 14089-14098.

Work funded by the McKnight and Baxter Foundations and grants from NIH.

Where applicable, the authors confirm that the experiments described here conform with The Physiological Society ethical requirements.

SA11

Sensory neuron mechanotransduction, mechanisms and molecules

G.R. Lewin

Neuroscience, Max-Delbrück Center for Molecular Medicine, Berlin, Germany

Somatic sensation is overwhelmingly felt as the result of mechanical stimulation or movement of the body or its parts. Indeed almost all tissues of the body receive an innervation from the peripheral axons of mechanosensitive sensory neurons with their cell body in the dorsal root or trigeminal ganglia. Remarkably, the mechanisms and molecules used by sensory neurons to transform mechanical force into an electrical signal are poorly understood. We term this process sensory neuron mechanotransduction, to distinguish it from mechanotransduction in the specialized epithe-

lial hair cells of the inner ear. It is assumed that specialized mechanosensitive ion channels that are gated by force, underlie a graded receptor potential in sensory afferent endings. The graded receptor potential leads to action potential firing that decodes the stimulus magnitude. We have sought to be able to measure mechanosensitive currents in isolated sensory neurons in acute culture that presumably underpin the receptor potential. We have found two main types of highly sensitive mechanosensitive currents in the neurites and somas of sensory neurons (Lechner et al. 2009; Hu et al. 2010). These two currents have been termed rapidly-adapting and slowly adapting mechanosensitive currents. The rapidly adapting (RA-type current) is found in all mechanoreceptors but also in a substantial number of nociceptors and this current inactivates very rapidly. The slowly adapting current (SA-type) has a distinct pharmacology and biophysical profile from the RA-type current and is only found in nociceptive sensory neurons. The relevance of mechanosensitive currents for in vivo mechanosensitivity has been demonstrated by experiments showing that such currents are absent in neurons with a targeted disruption of the gene encoding the integral membrane protein called stomatin-like protein-3 (SLP3) (Wetzel et al, 2007). In SLP3 mutant mice a substantial number of sensory afferents in the skin completely lack mechanosensitivity. Recently we have addressed the mechanism by which the mechanosensitive current is activated in sensory neurons. In principle the current could be activated by membrane stretch or, analogous to the hair cell, an extracellular tether might transfer force from the matrix directly to the channel. We have used a variety of tools to manipulate extracellular proteins including limited proteolysis and combined physiological measurements with quantitative transmission electron microscopy. These experiments show that the presence of an extracellular tether protein filament with a length of 100 nm appears to be necessary for gating the RA-type current (Hu et al. 2010). The tether molecule is synthesized by sensory neurons and binds to a laminin-containing matrix. Our data is the first to show that a tether gating mechanism is relevant for somatic sensory neurons. Interestingly, activation of the SA-type current does not appear to depend on a link to the extracellular matrix. I will also present new data that the sensitivity of mechanosensitive channels in sensory neurons is maintained by unconventional motor proteins.

Lechner SG, Frenzel H, Wang R and Lewin GR. (2009). Developmental waves of mechanosensitivity acquisition in sensory neuron subtypes during embryonic development. *EMBO J* 28, 1479-1491.

Wetzel C, Hu J, Riethmacher D, Benckendorff A, Harder L, Eilers A, Moshourab R, Kozlenkov A, Labuz D, Caspani O, Erdmann B, Machelska H, Heppenstall PA and Lewin GR. (2007). A stomatin-domain protein essential for touch sensation in the mouse. *Nature* 445, 206-209.

Hu J, Chiang LY, Koch M, and Lewin GR Evidence for a protein tether involved in somatic touch. *EMBO J*. 2010 Feb 17;29(4):855-67

Funding has been obtained from the Deutsche Foorschungsgemeinschaft collaborative resaerch center 665

Where applicable, the authors confirm that the experiments described here conform with The Physiological Society ethical requirements.

Vesicle traffic in hair cells and the coding problem in the mammalian cochlea

J. Ashmore

University College London, London, UK

There are two types of mechanosensitive hair cell in the mammalian cochlea: outer hair cells (OHCs), implicated in mechanical tuning of the sound responsiveness of the basilar membrane, and inner hair cells (IHCs), the primary sensory end cells of the auditory nerve fibres. The two cell types are distinguishable morphologically, by the organization of their stereocilial bundle and by their position within the organ of Corti. Both types of hair cell are innervated by afferent dendrites through ribbon synapses, with OHC and IHC pathways projecting to different brainstem targets. In the mouse cochlea, each IHC contacts between 10 and 20 afferent dendrites, depending on cochlear position, and it has been a long-standing problem to identify the significance of this signal pathway divergence. In order to study possible functional differences between individual ribbon synapses in IHCs, we have developed imaging techniques using two photon laser scanning confocal microscopy to look into the organ of Corti in the isolated temporal bone, (Griesinger et al, 2005). Using FM1-43 as marker of intracellular vesicle and membrane trafficking from the apex to the base of mouse IHCs, we found it possible to identify regions of intense fluorescence, each about 200-500 nm in diameter, localized at the base of each IHC. Such regions are candidate sites of vesicle aggregation around the ribbon. Combined with whole cell patch clamp recording, individual calcium entry sites around the cell's basal pole could also be detected using conventional calcium indicators (e.g OGB-5N) added through the patch pipette. On depolarization of an IHC from -70 to -10 mV, calcium increased in tightly controlled regions ('hotspots') near the basal pole of the IHC. Up to five spots could be imaged simultaneously in any one plane. The kinetics showed a rapid rise to a peak and decay with a time constant of ca. 200 ms. The positions of such calcium signals were compatible with colocalisation of calcium entry and the ribbon structures. Individual responses varied in amplitude from one side of the IHC to the other. In mean, 34% larger amplitude responses were found on the modiolar side as compared to the pillar side of the cell. The mechanism underlying this difference is not clear, but is likely to correlate with the distinction between the sites of origin of high and low threshold auditory nerve fibres terminating on the IHCs found in other species (Liberman, 1982). This heterogeneity of synaptic properties has been implicated explaining how a full range of sound intensities can be encoded by the cochlea.

Griesinger, C.B. et al Fast vesicle replenishment allows indefatigable signalling at the first auditory synapse. *Nature*. 2005. 435, 212-5.

Liberman, M.C. Single-neuron labeling in the cat auditory nerve. *Science*. 1982. 216, 1239-41.

Supported by Eurohear, the Fondation de l'Ecole Normale Supérieure and The Physiological Society.

Where applicable, the authors confirm that the experiments described here conform with The Physiological Society ethical requirements.

SA15

GABAergic inhibition contributes to the rapid adaptation process of Pacinian corpuscle

L. Pawson

Institute for Sensory Research, Syracuse University, Syracuse, NY, USA

Pacinian corpuscles (PCs) are tactile receptors composed of a nerve ending (neurite) that is encapsulated by layers of lamellar cells. PCs are classified as primary mechanoreceptors because there is no synapse between the transductive membrane and the site of action potential generation. These touch receptors respond in a rapidly adapting manner to sustained pressure (indentation or displacement), which until now was believed to be attributable solely to the mechanical properties of the capsule. The hemi-lamellar cells of the capsule, which lie closest to the nerve, stem from Schwann, or glial cells. In the last decade, a number of neuroscientists have shown that glial cells can play an active role in communicating with neurons and vice versa. Evidence of positive immunoreactivity for GABA receptors on the neurite, as well as evidence for gene expression of synaptobrevin in the lamellar cells led to the hypothesis that GABAergic inhibition originating from the lamellar cells is involved in the rapid adaptation process of PCs. Electrophysiological data from isolated PCs demonstrates that, in the presence of either gabazine or picrotoxin (GABA receptor antagonists), many action potentials appear during the static portion of a sustained indentation stimulus (similar to slowly adapting receptors) and that these static spikes completely disappear in the presence of GABA. It was consequently hypothesized that glutamate, released by either the neurite itself or the lamellar cells, caused these action potentials. Indeed, the glutamate receptor blocker kynurenate either decreased or totally eliminated the static spikes. Together, these results suggest that GABA, emanating from the modified Schwann cells of the capsule, inhibits glutamatergic excitation during the static portion of sustained pressure, thus forming a “mechanochemical,” rather than purely mechanical, rapid adaptation response. While this kind of glial–neuronal interaction has been found in other peripheral sensory organs (Pack and Pawson, 2010), it is a completely novel finding for the PC (Pawson et al., 2009). We believe that understanding the PC rapid adaptation process in more detail is important because this touch receptor is found only in higher vertebrates and as such has an adaptive significance. The ability to adapt very rapidly to touch stimuli makes the Pacinian corpuscle a wonderful detector of vibrations in the environment. This gives higher mammals a better opportunity to detect prey or predators. Elephants can communicate with other elephants from distances up to 16–30km away, by detecting vibrations in the ground with their feet. A better understanding of the chemical interaction between the glial cells of the PC capsule and its nerve ending during rapid adaptation will give scientists of the future

the ability to re-create this important ability to feel vibrations in prosthetic hands, feet, fingers and toes.

Pack AK and LJ Pawson (2010) Neuroglial modulation in peripheral sensory systems. *The Neuroscientist* 16: 342-348, first published on January 8, 2010 doi:10.1177/1073858409356113

Pawson L, LT Prestia, GK Mahoney, B Güçlü, PJ Cox and AK Pack (2009) GABAergic/glutamatergic–glial/neuronal interaction contributes to rapid adaptation in Pacinian corpuscles. *J Neurosci* 29: 2695-2705.

Where applicable, the authors confirm that the experiments described here conform with The Physiological Society ethical requirements.

SA16

The role of synaptic-like vesicles in control of mechanosensation in peripheral nerve terminals

G. Bewick¹ and R. Banks^{2,1}

¹University of Aberdeen, Aberdeen, UK and ²Durham University, London, UK

Small (50 nm dia), clear vesicles in vertebrate primary mechanosensory nerve terminals were identified by early electron microscopists - at about the same time as in synaptic terminals. This was recognised by Sir Bernard Katz, in *Nerve, Muscle and Synapse* (1966) but the absence of an obvious mechanosensory function and the keen interest in their role at synapses meant they were largely forgotten. Recently, however, we have become intrigued by the ubiquitous presence of these 'synaptic-like vesicles' (SLVs) on the 'wrong' side of peripheral mechanosensory nerve/target contacts – i.e. in sensory terminals that receive and transduce mechanosensory stimuli. This includes muscle spindle afferents, hair follicle palisade endings, atrial and aortic baroreceptors, and joint proprioceptors – indeed, any mechanosensory nerve terminals that have been studied ultrastructurally. The resemblance between SLVs and synaptic vesicles is more than simply structural (for original references, see Bewick et al, 2005). Peripheral mechanosensory terminals contain synaptobrevin/VAMP I and II, synapsin I, synaptophysin, the terminal membrane docking protein syntaxin IB, even glutamate and vGlut1. Crucially, function is disrupted by the synaptic neurotoxins tetanus toxin and latrotoxin, and Ca channel blockers. However, there are important differences. SLVs are not 'synaptic', since release sites ('active zones'), if present, are poorly developed and SLVs recycle over the whole terminal surface. We are investigating the role of SLVs in primary mechanosensory terminals, in particular their mechanism of action and their potentially essential importance in controlling the functional expression of the stretch-activated channels in the terminal membrane. We initially used the rat muscle spindle primary endings as a model (Bewick et al, 2005), but the principles uncovered seem essentially the same in the other mechanosensory terminals we have examined – lanceolate terminals of palisade endings of guard hair and vibrissal follicles; and aortic baroreceptors. Evidence will be presented that SLVs undergo endo- and exocytosis, in a Ca-

dependent and mechanically modulated manner. We also have evidence they release glutamate which regulates terminal firing by activating an established but highly unusual metabotropic glutamate receptor (mGluR; (Boss et al, 1994; Pellegrini-Giampietro et al, 1996). The mGluR is insensitive to common ionotropic and metabotropic receptor antagonists, but is inhibited by the group I mGluR agonist (R,S) 3,5 DHPG and a selective antagonist, PCCG-13 (Pellicciari et al, 1999). Indeed, receptor inhibition alone can totally block mechanically evoked output. In the hippocampus, the mGluR activates phospholipase D (Pellegrini-Giampietro et al, 1996), so we term it the PLD-mGluR, pending official characterisation. The data indicate SLVs recycle tonically, releasing glutamate, while mechanical activity increases recycling. The antagonist pharmacology suggests endogenous glutamate release acts through a non-canonical, PLD-mGluR to maintain excitability in these sensory endings. This glutamatergic system, therefore, may be a ubiquitous autogenic modulator of mechanosensory peripheral terminals, powerfully modulating the mechanically-evoked output of the transduction process, between total abolition and a doubling of afferent firing.

Bewick GS, Reid B, Richardson C & Banks RW (2005). Autogenic modulation of mechanoreceptor excitability by glutamate release from synaptic-like vesicles: Evidence from the rat muscle spindle primary sensory ending. *J Physiol* 562, 381-394.

Boss V, Nutt KM & Conn PJ (1994). L-cysteine sulfinic acid as an endogenous agonist of a novel metabotropic receptor coupled to stimulation of phospholipase D activity. *Molecular Pharmacology* 45, 1177-1182.

Katz B (1966). *Nerve, muscle and synapse*. p98. McGraw-Hill, London.

Pellegrini-Giampietro DE, Torregrossa SA & Moroni F (1996). Pharmacological characterization of metabotropic glutamate receptors coupled to phospholipase D in the rat hippocampus. *Br J Pharmacol* 118, 1035-1043.

Pellicciari R, Marinozzi M, Costantino G, Natalini B, Moroni F & Pellegrini-Giampietro D (1999). (2R,1'S,2'R,3'S)-2-(2'-carboxy-3'-phenylcyclopropyl)glycine (PCCG-13), the first potent and selective competitive antagonist of phospholipase D-coupled metabotropic glutamate receptors: Asymmetric synthesis and preliminary biological properties. *J Med Chem* 42, 2716-2720.

Where applicable, the authors confirm that the experiments described here conform with The Physiological Society ethical requirements.

SA17

Transduction, adaptation and encoding in spider mechanoreceptors

A. French

Dalhousie University, Nova Scotia, NS, Canada

Arthropods have provided several important models of mechanotransduction. In contrast to vertebrate somatic receptors, arthropod cuticular receptors have cell bodies located close to their sensory endings, facilitating electrophysiological and morphological studies. Spider slit sensilla provide a useful general model of spiking mechanoreceptors in which the neurons can be visualized during experiments,

and are easily accessible to chemical changes in the bathing saline. Electrical recording, including single-electrode voltage-clamp is possible during simultaneous mechanical stimulation of the slits, which allows the receptor current, receptor potential and action potentials to be measured. The neurons also receive peripheral efferent innervation from the CNS that affects the mechanosensory processes at several stages, providing an important model of sensory neuromodulation. Spiders have many slit sensilla, but the VS 3 organ in the spider patella has been most widely used (Barth 1971; French et al. 2002). VS 3 neurons respond to stress in the cuticle with rapidly adapting action potentials. Although their physiological functions are unknown, they probably act primarily as vibration detectors. The spider sensory world has a large mechanical component, and vibration is clearly important for functions such as prey detection and courtship. Receptor current in VS 3 neurons is highly selective for sodium ions and can be increased by extracellular acid, suggesting that the mechanotransduction channels are members of the Acid-sensitive/Degenerin/Epithelial sodium channel family. Immuno-labelling with antibodies to the *C. elegans* MEC 4 protein supports this hypothesis. Several lines of evidence suggest that the mechanotransduction channels are located at the tips of the sensory dendrites, and that action potentials are initiated in the same region. The number of active mechanotransduction channels per neuron has been estimated to be five hundred. VS 3 neuron membranes have a voltage-sensitive T type calcium current that activates when the neurons are depolarized above about 50 mV (normal resting potential is about 70 mV). Antibody labelling to the CaV3.1 encoded $\alpha 1G$ sub-unit indicated that voltage-activated calcium channels are widely distributed over all major regions of the neurons. Mechanically-driven receptor current does not depolarize the neurons enough to activate a calcium current, but action potentials cause large increases in internal calcium concentration. Calcium elevation, in turn, reduces receptor current, possibly by binding to mechanotransduction channels, with an estimated stoichiometry of two calcium ions per channel. This indicates that calcium concentration serves as a feedback regulator of mechanical sensitivity. Mechanical information is transmitted to the CNS by action potentials. Quantitative measurements of information capacity and action potential entropy as a function of firing rate indicate that VS 3 neurons have a low level of inherent noise, and that information transmission is limited primarily by the maximum firing rates that the neurons can achieve.

Barth FG (1971) Der sensorische apparat der spaltsinnesorgane (*Cupiennius salei* Keys., araneae). *Z Zellforsch* 112: 212-246.

French AS, Torkkeli PH, Seyfarth E-A (2002) From stress and strain to spikes: mechanotransduction in spider slit sensilla. *J Comp Physiol A* 188: 739-752.

Where applicable, the authors confirm that the experiments described here conform with The Physiological Society ethical requirements.

A

Aaron, J.E. C08 and PC08
Abuhamdah, R. PC41*
Affleck, V.S. PC27*
Allen, G. C09 and PC09
Anirudhan, G. C10 and PC10
Arnold, S. PC31
Aryiku, C. PC22
Ashmore, J. SA14*
Ashworth, R. PC25*
Atherton, J. PC31

B

Baker, J.S. PC36
Bakker, A. SA09*
Banks, R. SA16
Banks, R.W. C15 and PC15, PC22, PC39
Beech, D. SA02*
Berna-Erro, A. PC29
Bewick, G. SA16*
Bewick, G.S. C15 and PC15, PC22, PC39
Blanchard, M.G. C03 and PC03*
Bohlender, J. C16 and PC16
Boillat, A. C01 and PC01*
Bouchelouche, P. C05 and PC05
Breen, C. PC41
Burkholder, T. SA04*
Burroughs, S.L. PC34

C

Carroll, M. PC41
Chapple, P. PC35
Chazot, P. PC41
Chazot, P.L. PC32, PC34
Connolly, W. PC41
Cork, S.C. PC32*
Crouch, R.S. C04 and PC04

D

Davies, B. PC36
Davis, C. PC35*
de Nooij, J.C. PC39*
Dionisio, N. PC26*
Dixon, C. PC41
Doobar, S. PC39
Dosenko, V. C06 and PC06
Drummond, H. SA05*
Duan, X. PC31*
Duggett, N.A. PC34*

E

Elias, S.O. PC24*
Ellis, E.M. PC21
Evans, P.J. PC36

F

Fallon, V. C08 and PC08
Fedirko, N. PC38
Fettiplace, R. C13 and PC13,
C14 and PC14
French, A. SA17*
Frenzel, H. C16 and PC16*
Fullard, N. PC37
Furness, D.N. C14 and PC14*

G

Gallant, A.J. PC31
Garner, P.E. C08 and PC08*
Getting, S.J. PC40, PC33
Gilligan, L.C. PC30
Goodman, M.B. SA10*
Grace, F.M. PC36
Grachev, P. PC19*
Graham, M.R. PC36*
Grifoni, S. SA05
Gross, M. C16 and PC16

H

Hackney, C.M. C13 and PC13*,
C14 and PC14
Han, S.Y. PC41
Harris, J. C09 and PC09
Haycraft, C.J. C07 and PC07
Heydari, A. C04 and PC04
Hoehner, T. PC37
Honore, E. SA03*
Hoskin, I. PC41
Howes, M.J. PC41
Huang, L. PC41
Hucklebridge, F. PC33

I

Ismail, N. C18 and PC18*
Ivanova, I. C06 and PC06

J

Jaja, S.I. PC24
Jardin, I. PC26
Jessell, T.M. PC39
Johnstone, S. C04 and PC04, PC31
Jordan, J. C02 and PC02

K

Karunarathna, U. PC25
Kellenberger, S.C01 and PC01, C03 and PC03,
SA01*
Kelly, S. C09 and PC09*
Kerrigan, M.J. PC33, PC40
Kinsey-Jones, J.S. PC19
Klaerke, D.A. C05 and PC05
Knight, M. PC35
Knight, M.M. C07 and PC07
Kocher, S. C12 and PC12*
Kopach, O. PC38
Krivcevska, C. PC25

L

Lahne, M. PC25
Land, S.C. C18 and PC18, PC23
Lapatsina, L. C02 and PC02
Larsen, T. C05 and PC05
Lechner, S.G. C02 and PC02*,
C10 and PC10
Lees, G. PC41
Lewin, G.R. C02 and PC02,
C10 and PC10, C11 and PC11, C16 and
PC16, SA11*
Li, X.F. PC19
López, E. PC20*, PC29
Lucas, M.L. PC30*
Luft, F.C. C02 and PC02

M

Mahendrasingam, S. C13 and PC13,
C14 and PC14
Mahita, M. PC41
Mansley, M.K. PC28
Markworth, S. C02 and PC02
McDonagh, T. C17 and PC17*
McGlashan, S.R. C07 and PC07
McMaster, T.J. C12 and PC12
Mickael, M.E. C04 and PC04*
Morrison, J.D. PC30

N

Nedelcheva, Y. PC40*
Netsyk, O. PC38*
Noordin, L. PC21*
Novokhatska, T. C06 and PC06*

O

O'Byrne, K.T. PC19
Ødum, L. C05 and PC05
Omerbasic, D. C10 and PC10

P

Parker, E.L. PC33*
Pawson, L. SA15*
Peetrooms, C. PC33
Pilz, R. SA08*
Pinsker, K. C16 and PC16
Poole, C.A. C07 and PC07
Poole, K. C02 and PC02, C11 and PC11*
Pyner, S. C04 and PC04, PC27,
PC31, PC32

R

Rahbek, M. C05 and PC05*
Redondo, P.C. PC20, PC26, PC29*
Reichelt, J. PC37*
Rizner, T. PC21
Robert, D. C17 and PC17
Rosado, J.A. PC20, PC26, PC29
Rosamond, M.C. PC31
Rosenbaum, S.T. C05 and PC05

S

Salido, G.M. PC20, PC26, PC29
Shenton, F.C. C15 and PC15*
Sheppard, D.N. C12 and PC12
Simon, A. PC39
Simpson, S. PC28*
Skerry, T. SA07*
Smith, E.S. C02 and PC02
Sofola, O.A. PC24
Soloviev, A. C06 and PC06
St. John Smith, E. C10 and PC10*
Stec, D. SA05
Steel, K.P. PC39

T

Tickle, J.A. C14 and PC14
Tishkin, S. C06 and PC06

U

Umoren, G.A. PC24

V

Vollmers, A. PC37

W

Wann, A.K. C07 and PC07*
Watson, S. PC22*
Watt, G.B. PC23
Whitelaw, C. PC30
Wilson, S.M. C18 and PC18, PC23*, PC28
Windmill, J. C17 and PC17

Wynne, P.J.PC30

Z

Zbidi, H.PC26